8

ENSO Low-Frequency Modulation and Mean State Interactions

Alexey V. Fedorov[1,2], Shineng Hu[3], Andrew T. Wittenberg[4], Aaron F. Z. Levine[5], and Clara Deser[6]

ABSTRACT

Is El Niño changing with global warming? Can we anticipate decades with extreme El Niño events? To answer these questions confidently, we need to understand the modulation of the El Niño Southern Oscillation phenomenon (ENSO) that occur on decadal and multidecadal timescales and involve changes in El Niño amplitude, periodicity, dominant "flavors", shifts in the Intertropical Convergence Zone, and other properties. As major progress has been made in understanding various factors that can affect these characteristics of El Niño, two main paradigms have emerged to explain the observed modulation of ENSO: (i) internally generated variations due to the chaotic nature of the ocean-atmosphere coupled system and (ii) externally driven variations due to cyclic or secular changes in the properties of the tropical background state such as mean winds or ocean thermocline depth. This article reviews these two paradigms in the context of available observations, idealized models, and comprehensive general circulation models describing El Niño. Which paradigm will dominate in the coming decades and whether global warming is already affecting El Niño remains unclear.

8.1. INTRODUCTION

With the continuing progress in observing and understanding El Niño over the past two decades (e.g. Meinen & McPhaden, 2000; Fedorov & Philander, 2000, 2001; Fedorov et al., 2003; Lengaigne et al., 2006; Jin et al., 2003, 2006; Guilyardi et al., 2009, 2012b; Collins et al., 2010; Wittenberg, 2009; Vecchi & Wittenberg, 2010; McPhaden et al., 2011; Capotondi et al., 2015a; Takahashi & Dewitte, 2016; C. Wang et al., 2017; Santoso et al., 2017;

Hu & Fedorov, 2017a, 2018; Xie et al., 2018; Timmermann et al., 2018; and many other important studies), it has become apparent that each El Niño event is unique and that ENSO variability as a whole undergoes pronounced decadal and multidecadal modulations. These modulations involve changes in El Niño amplitude, periodicity, the propagation direction of SST anomalies, the dominating El Niño "flavors," the behavior of the Intertropical Convergence Zone (ITCZ), and changes in other El Niño properties as well as global impacts and teleconnections.

These climate modulations are evident in the observational SST record of the past 150 years (Figure 8.1). For example, ENSO variability of moderate intensity was typical of the late 19th and early 20th centuries, which was followed by very weak variability in the 1930s and 1940s (with the standard deviation of Niño3 index, STD ≈ 0.5°C). The gradual growth in ENSO amplitude since the 1950s resulted in two decades of particularly strong ENSO: the 1980s and 1990s (STD ≈ 0.9°C). Those two decades saw the two strongest El Niño events of the observational record to date: the extreme events of 1982

[1] *Earth and Planetary Sciences, Yale University, New Haven, CT, USA*

[2] *LOCEAN/IPSL, Sorbonne University, Paris, France*

[3] *Lamont-Doherty Earth Observatory, Columbia University, Palisades, NY, USA*

[4] *NOAA Geophysical Fluid Dynamics Laboratory, Princeton, NJ, USA*

[5] *Department of Atmospheric Sciences, University of Washington, Seattle, WA, USA*

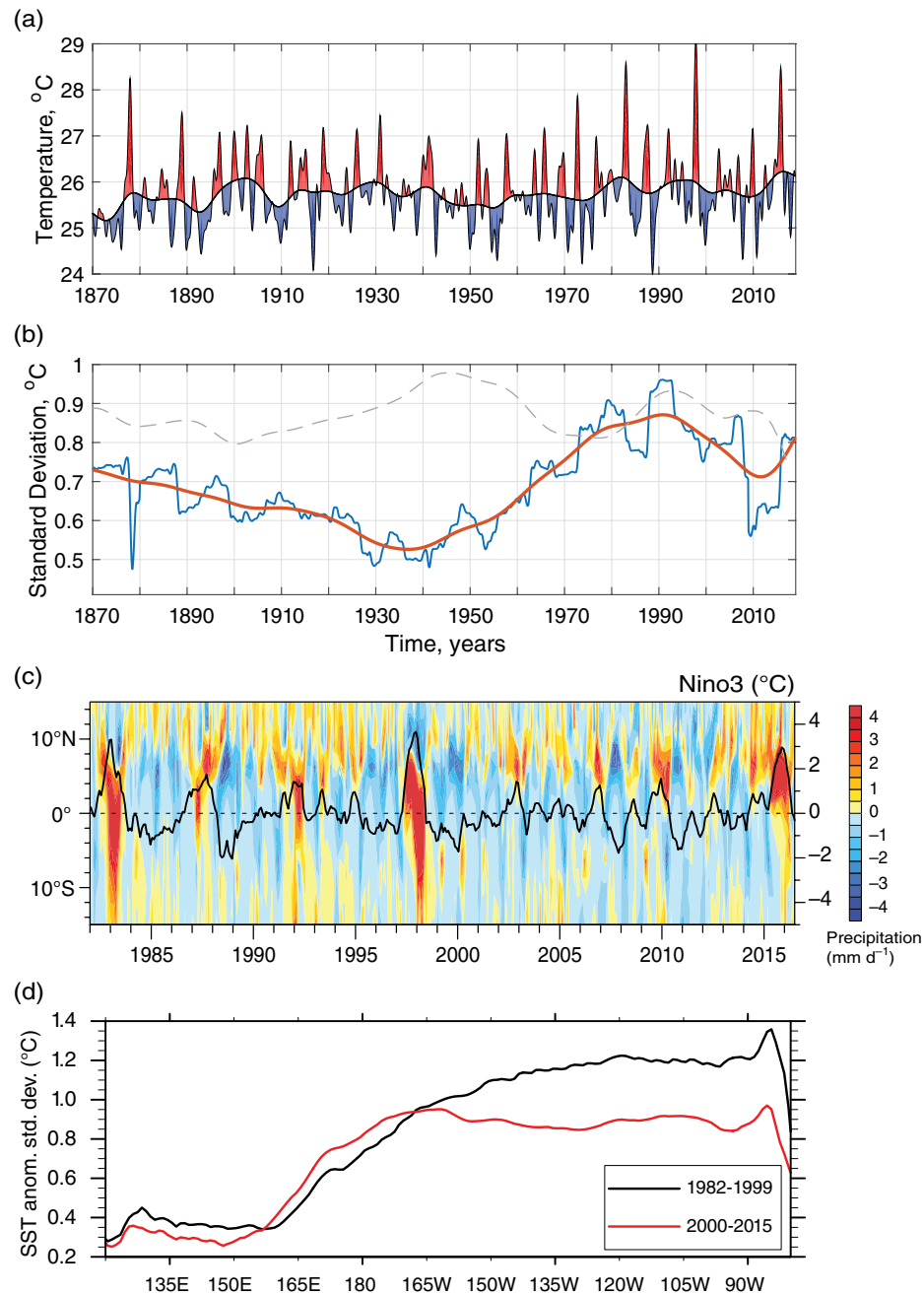[6] *NCAR, Climate and Global Dynamics Division, Boulder, CO, USA*

Figure 8.1 (a) Interannual variations in sea surface temperatures (SST) in the eastern equatorial Pacific Niño3 region (5°S–5°N, 150°W–90°W) shown on the background of decadal changes (in °C). El Niño conditions correspond to warmer temperatures. Note El Niño events of 1982, 1997, and 2015, the strongest in the instrumental record. The annual cycle and higher-frequency variations are removed from the data. The baseline is obtained by applying a decadal low-pass filter to the data. Updated after Fedorov and Philander (2000). (b) Standard deviation of the above record computed as a 20-year running mean (blue line). The red line shows this data after smoothing. The dashed line shows smoothed variations in standard deviation for the Niño3 SST annual cycle. (c) A Hovmoller diagram of eastern Pacific precipitation anomalies averaged within 150°W–90°W since 1982; Niño3 variations are also shown (black line, in °C, axis on the right). (d) Standard deviation of SST anomalies along the equator (averaged 5°S–5°N) for two intervals: the 1980s and 1990s vs the early 21st century. After Hu and Fedorov (2018).

and 1997, which occurred as part of the much-discussed climate shift of the late 1970s that affected many components of the climate system (e.g. Fedorov & Philander, 2000, Meehl et al., 2009). A multicomponent linear inverse model has confirmed that statistically significant systemic changes did occur in ENSO dynamics in the early 1980s (Capotondi & Sardeshmukh, 2017).

The regularity and periodicity of events have also been changing through time. One can notice the clockwork development of El Niño in the early 20th century with warm events happening every 3 years, rare and irregular El Niño occurrence in the mid 20th century, and then exceptionally strong events separated by about 5 years in the 1980s and the 1990s. Since the power spectrum of ENSO variability has a broad peak with a maximum at about 3–5 years (e.g. Deser et al., 2009; Manucharyan & Fedorov, 2014), one cannot conclude without any additional assumptions whether these variations are random or forced by external factors. While the cold phase of the oscillation, La Niña, varies broadly as well, ENSO modulations arise primarily from variations in the characteristics of El Niño.

The first two decades of the 21st century produced relatively weak El Niño events with the exception of the strong event of 2015 (Figure 8.1). This can be interpreted as another climate shift of the early 2000s that went in the opposite direction to what happened in the latter 1970s. During 2000–2014 the Niño3 STD was reduced by 20%–30% relative to the previous two decades. This ENSO weakening has been accompanied by a shift from stronger eastern Pacific (EP) El Niño events to weaker central Pacific (CP) events, which have their maximum SST anomaly located farther west (Ashok et al., 2007; Kug et al., 2009; Kao & Yu, 2009; see Figure 8.1d and chapter 4 of this book for more detail).

Furthermore, the ITCZ precipitation band, whose mean climatological position is north of the equator and which would typically migrate towards the equator during EP El Niño events, failed to do so during the El Niños of 2000–2016 (Figure 8.1c; Hu & Fedorov, 2018). Other terminologies for CP and EP El Niño events are also used, for example, El Niño Modoki versus conventional El Niño (Ashok et al., 2007) or warm pool versus cold tongue El Niño (Kug et al., 2009). The global impacts of CP and EP events differ significantly (chapter 4 and section VI of this book). While the 2015–2016 El Niño is considered an EP event based on its extreme warming magnitude in the eastern Pacific (Levine & McPhaden, 2016; Hu & Fedorov, 2017a), it shared properties of both types throughout its development (Hu & Fedorov, 2017a; Santoso et al., 2017).

Concurrently with the weakening of El Niño, the tropical Pacific experienced a negative phase of the Interdecadal Pacific Oscillation, characterized by a broad cooling in the eastern tropical Pacific and stronger trade winds (England et al., 2014). In addition, the mean cross-equatorial southerly winds in the eastern Pacific also strengthened

significantly (Hu & Fedorov, 2018). These mean state changes and the ENSO weakening may be connected, but which one causes the other remains debatable, as ENSO modulations themselves can cause changes in the mean state (Ogata et al., 2013). The issue is how to distinguish this nonlinear rectification of El Niño/La Niña signals onto the mean state and any independent mean state changes that can cause ENSO modulations (the subject of the next two sections). In other words, are decadal changes in the baseline in Figure 8.1a caused by ENSO rectification or by factors external to ENSO?

The overall strengthening of ENSO variability since the 1950s, which culminated in three extreme El Niño events, coincided with rapidly increasing atmospheric CO_2 concentration and rising global mean temperatures, which raises the question of whether this increase in El Niño amplitude could be due to global warming (Fedorov & Philander, 2000, 2001; Collins et al,, 2010; Cai et al., 2015; Capotondi & Sardeshmukh, 2017; also see chapter 13 of this book). To answer this question, we need to understand what causes ENSO modulations and also develop tools to distinguish those externally forced from internally generated, which would help detect emerging ENSO changes induced by global warming (e.g. Timmermann, 1999).

It is noteworthy that ENSO modulations are accompanied by modulations in the seasonal cycle in the tropics (dashed line in Figure 8.1b). Earlier studies noticed that ENSO activity and the strength of the annual cycle may be anticorrelated: strong ENSO would go together with a weak annual cycle and vice versa (e.g. Chang et al., 1994; Fedorov & Philander, 2001). Indeed, the interval of weak ENSO in the mid-20th century coincides with the strongest annual cycle in the observations. However, the relationship between the strengths of ENSO and the annual cycle is not as straightforward, especially in the second half of the 20th century, and is further complicated by nonlinearities (Hannachi et al., 2003).

Strong ENSO modulations also occurred in the past on different timescales, as suggested by paleo records (e.g. Cobb et al., 2003; Cane, 2005; also see chapter 5), and observational and modeling evidence indicate that robust El Niños with different characteristics persisted across wide changes in climate (for a review see Manucharyan & Fedorov, 2014). Nevertheless, there are indications that ENSO variability during the second half of the 20th century might have been the strongest not only in the modern record but also in the entire Holocene (e.g. Cobb et al., 2013; McGregor et al., 2013; White et al., 2018). This makes the question of the effect of global warming on ENSO even more compelling.

Two main paradigms have emerged to explain the observed modulation of ENSO: (i) internally generated variations due to the chaotic nature of the atmosphere and/or the ocean-atmosphere coupled system in the equatorial Pacific and (ii) externally driven variations

due to longer-term cyclic or secular changes in the properties of the tropical background state such as the mean winds or ocean thermocline depth. A swinging pendulum provides a partial analogy. When randomly hit from different sides, a pendulum would typically exhibit alternating intervals with stronger or weaker amplitude of motion. As long as we consider the random forcing as part of the dynamics of the pendulum, this scenario is similar to the first paradigm. Now, if one starts gradually changing the length of the pendulum, that will also modulate the motion. This latter example is related to the second paradigm. Here, we will review these two paradigms in the context of available observations, idealized models, and comprehensive general circulation models (GCM) describing El Niño. It is noteworthy that whether ENSO modulations are externally forced or internally generated typically cannot be assessed solely based on the relatively short observational records; therefore, many of our conclusions will rely on models of various complexities.

8.2. INTRINSICALLY GENERATED MODULATION OF ENSO

8.2.1. Decadal Modulation of ENSO in Idealized Models

Given the challenges of understanding the causes of multidecadal variability of ENSO in the observed record and in comprehensive GCMs, models of reduced complexity are broadly used to help interpret the observations and understand the different potential causes of this multidecadal variability (chapter 6). In such models, decadal modulation can arise as part of linear or quasi-linear dynamics if the dominant internal ENSO mode is weakly damped or slightly unstable with stochastic forcing (e.g. Kirtman & Schopf 1998; Thompson & Battisti, 2000, 2001; Fedorov, 2002; Fedorov et al., 2003; Philander & Fedorov, 2003; Flügel et al., 2004) or as part of nonlinear dynamics of a low-order deterministic chaotic system (e.g. Tziperman et al., 1995; Jin et al., 1996; Timmermann et al., 2003; Roberts et al., 2016). Low-order deterministic chaos means that the system can be described by several ordinary differential equations exhibiting chaotic behavior such that small changes in initial conditions at finite times lead to a different solution without any noise forcing (e.g. Lorenz, 1963; Saltzman, 1962).

The simplest theoretical models of ENSO are linear and stochastically forced. The imposed stochastic forcing reflects the effect of westerly and easterly wind bursts (or surges) that frequently occur in the western/central tropical Pacific (e.g. Fedorov, 2002; Harrison & Chiodi, 2009; Hu et al., 2014; Fedorov et al., 2015; D. Chen et al., 2015; Hu & Fedorov, 2016, 2017a; Levine et al., 2017a) and other atmospheric and oceanic high-frequency processes.

However, without additional modifications, these simple models struggle to replicate a key feature of ENSO – its

asymmetries. The SST anomalies for El Niño tend to be stronger, shorter in duration, and transition more robustly into the opposite phase (La Niña) than the corresponding SST anomalies for La Niña (Okumura & Deser, 2010; K.-Y. Choi et al., 2013; DiNezio & Deser, 2014; also see chapter 7). The El Niño/La Niña amplitude asymmetry, which is reflected in a positive skewness of about 0.85 of the SST timeseries in Figure 8.1a, varies greatly with the multidecadal modulation of ENSO. When extending conceptual models to account for the asymmetry, nonlinearity is added to the equations. In stochastically forced models, nonlinearity can be added as state-dependent noise (Eisenman et al., 2005; Levine & Jin, 2010; Levine et al., 2016) or a nonlinear growth rate (K.-Y. Choi et al., 2013; Takahashi & Dewitte, 2016).

More complicated nonlinear formulations of the dynamics can result in a low-order chaotic ENSO (B. Wang & Fang 1996; Timmermann et al., 2003; Mu et al., 2007). Earlier studies also emphasized nonlinear interactions between ENSO and the seasonal cycle to explain the chaotic behavior (Jin et al. 1994, Tziperman et al. 1994). We note, however, that in many of these low-order models without stochastic forcing, a transition to chaotic behavior typically requires unrealistically strong nonlinearity. Thus, ENSO is more commonly viewed as a weakly damped/slightly unstable low-frequency tropical coupled linear mode affected by moderate nonlinearity and sustained by stochastic wind forcing (Thompson & Battisti, 2000, 2001; Fedorov et al., 2003; Philander & Fedorov, 2003; or more recently Capotondi et al., 2018).

Examples of ENSO modulations generated by a diverse selection of simple models are shown in Figure 8.2, including a recharge oscillator with state-dependent noise forcing (Levine et al., 2016), a delayed oscillator with a nonlinear growth rate and noise forcing (K.-Y. Choi et al., 2013), and a low-order deterministic chaotic nonlinear oscillator (Mu et al., 2007). The recharge oscillator model generates an oscillation between SST in the eastern equatorial Pacific and mean thermocline depth described by two ordinary differential equations (Jin 1997, Meinen & McPhaden, 2000). The delayed oscillator is based on a differential equation for SST with an explicit time delay in one of the terms (Suarez & Schopf, 1988). The two oscillator models emerge as different approximations of an integrodifferential equation describing ENSO in a low-frequency limit (Fedorov, 2010). For further details, see chapters 6 and 7.

Given the asymmetries between El Niño and La Niña, observed changes in the tropical Pacific mean state on multidecadal timescales might be as simple as differences in rate of occurrence of large El Niño events (Schopf & Burgman, 2006; Ogata et al., 2013; Atwood et al., 2017). However, these changes in the mean state have been shown to influence ENSO growth rate and frequency (e.g. Fedorov & Philander, 2000, 2001; Wittenberg, 2002; Bejarano & Jin, 2008),
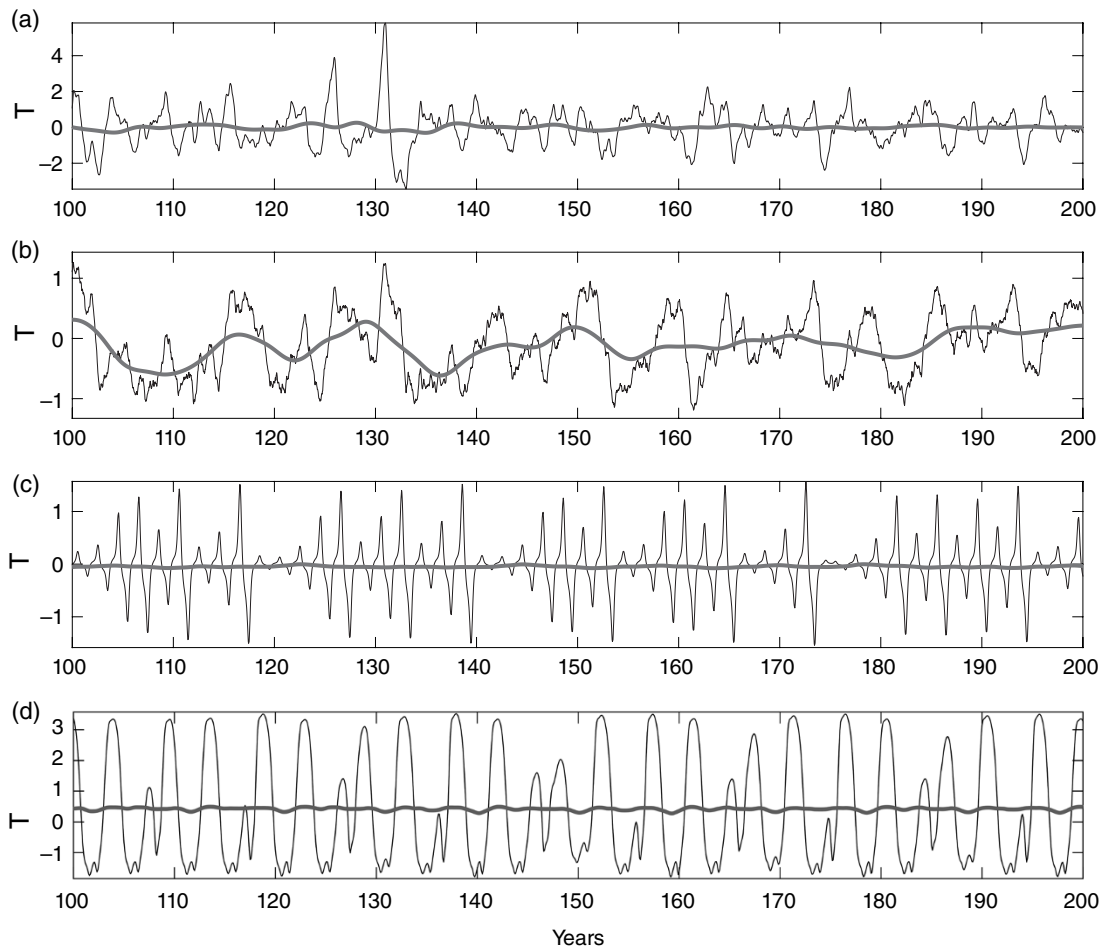
Figure 8.2 Examples of ENSO modulations in 100-year simulations of eastern equatorial Pacific SST anomalies (in °C) from different idealized models. (a) A recharge oscillator with state-dependent noise forcing (Levine et al., 2016), (b) a delayed oscillator with a nonlinear growth rate (K.-Y. Choi et al., 2013), (c) a low-order chaotic non-linear oscillator (Mu et al., 2007), and (d) a version of the Cane-Zebiak model (Bejarano & Jin, 2008). Black lines are 10-day outputs, grey lines are 11-year averages. For details, see text and chapters 6 and 7.

leading to potential feedbacks between changes in the mean state and changes in ENSO and making it difficult to separate forced and random changes in ENSO variability (Burgman et al., 2008). Noise-forced variability in ENSO is less predictable on decadal timescales where changes in the mean state are forced by the inherently random nature of the weather forcing being integrated by the ocean, which in turn modifies ENSO statistics by modulating the growth rate and frequency. Low-order deterministic chaos, on the other hand, suggests that there may be predictable modulations of ENSO on these decadal timescales depending on how well we know the initial conditions, as shown in the study of Karspeck et al. (2004) using the intermediate coupled model of Zebiak & Cane (1987), hereafter the Cane-Zebiak (CZ) model (see chapter 6).

The CZ model can produce a deterministically chaotic ENSO (e.g. Figure 8.2d), which is related to the existence of two unstable modes and strong nonlinearity in some of the model's versions. In the original nonlinear CZ

configuration, there are two distinct sets of phases of the multidecadal variability, one with a high ENSO variance and another with low ENSO variance, and the transitions from a low-variance state to a high variance state are more predictable than the transitions from high-variance to low-variance (Ramesh & Cane, 2019). Note, however, this result is different from the behavior of the GFDL CM2.1 general circulation model, which shows no clear predictability of decadal ENSO amplitude (see next section and Wittenberg et al., 2014).

In contrast to the original version of the CZ model, some newer configurations of this model have only one, weakly-damped mode and exhibit quasi-linear dynamics. Likewise, linear inverse modeling (LIM) of ENSO assumes that nonlinearities evolve fast enough to be treated as part of additive stochastic forcing in the LIM (Penland et al., 2000, Newman et al., 2016, and chapter 9). Consequently, it is unclear where on the spectrum between linear stochastic and low-order chaos the observations sit, and it is

possible that during some periods, ENSO is better simulated as a linear or quasi-linear stochastic system and others as a nonlinear low-order chaotic system. This issue has an important bearing on the behavior of comprehensive GCMs, as discussed next.

8.2.2. Decadal Modulation of ENSO in GCMs

Coupled GCM simulations have demonstrated that ENSO can undergo interdecadal modulations of its behavior, not unlike those seen in some simpler models, even in the absence of changes in external forcings. These modulations can emerge spontaneously, even in control runs where the external radiative forcing is held fixed (Rodgers et al., 2004, Wittenberg, 2009, Deser et al., 2012, Borlace et al., 2013, Vega-Westhoff & Sriver, 2017). An unforced control simulation described in Wittenberg (2009) and shown in Figure 8.3 exhibits strong intrinsic modulation of ENSO, with multidecadal epochs of very strong (epoch M7), weak (M5), regular (M2), or irregular

(M6) SST variability. The simulation can also generate epochs (e.g. M1 and M6) that resemble historical observations (e.g. R1 and R2), making it difficult to reject the model outright even if the simulated ENSO is generally stronger than observed. ENSO modulation is also evident in ensembles of historical simulations, where different ensemble members with identical external forcings can exhibit different ENSO behaviors during the same forcing decade (Newman et al., 2018).

Intrinsically generated modulation has been found to affect multiple aspects of ENSO: the amplitude, period, and spectrum (Wittenberg et al., 2006; Wittenberg, 2009; Stevenson et al., 2012; Borlace et al., 2013); spatio-temporal patterns (Wittenberg et al., 2014; Wittenberg, 2015; Capotondi et al., 2015a; C. Chen et al., 2017; Lee et al., 2014); teleconnections (Lee et al., 2016, 2018; Deser et al., 2017b), dynamical mechanisms and nonlinearity (Kug et al., 2010; Atwood et al., 2017), and predictability (Karamperidou et al., 2014; Wittenberg et al., 2014; Ding et al., 2018). The existence of strong intrinsic modulation
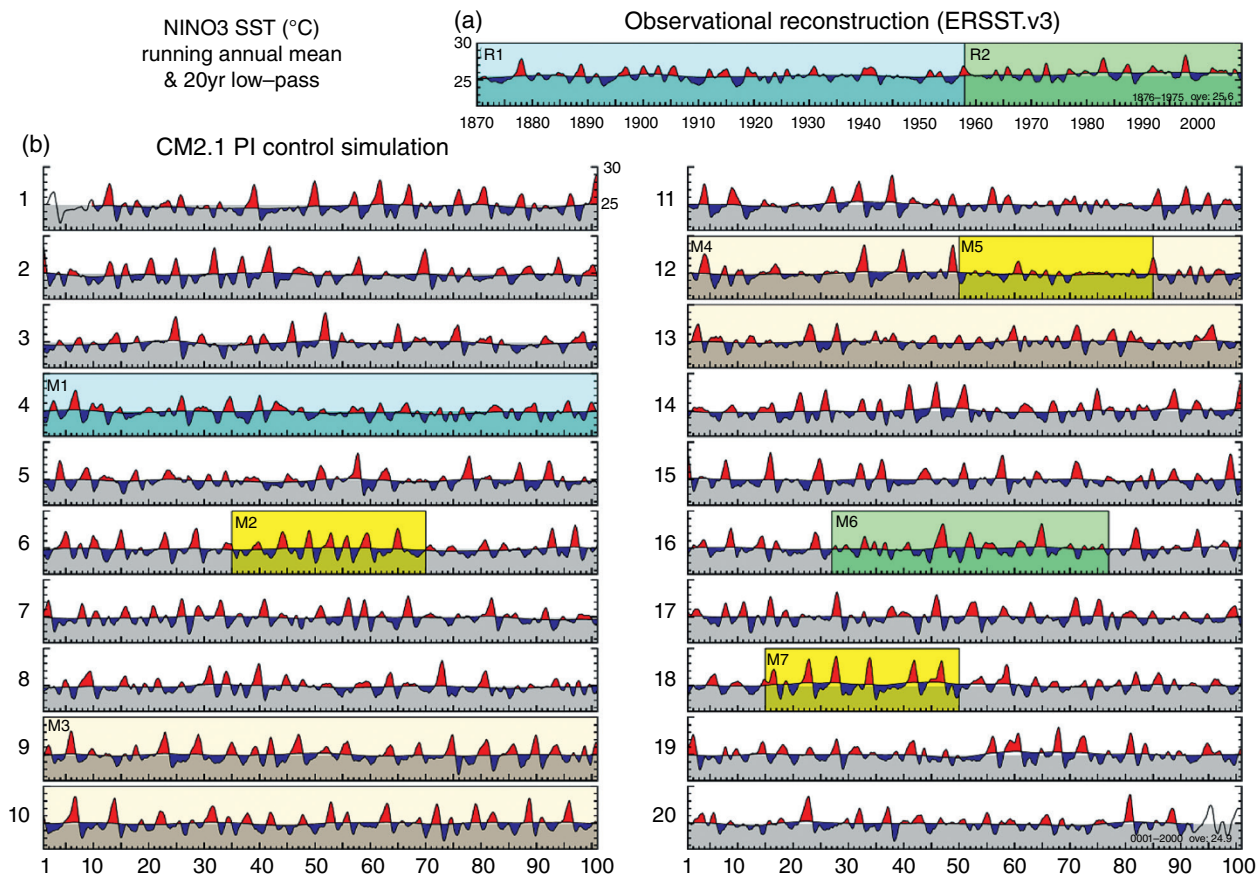

Figure 8.3 SST (°C) averaged over the Niño3 region (150°W–90°W, 5°S–5°N) from (a) the observational reconstruction of Smith et al. (2008) and (b) 20 centuries from the GFDL-CM2.1 preindustrial control run (Delworth et al., 2006; Wittenberg et al., 2006; Wittenberg, 2009). Red/blue shading highlights departures of the running annual-mean SST from a 20-year low-passed climatology. Gray shading indicates the 2000-year mean. Highlighted epochs (R1-2, M1-7) are discussed in the text. From Wittenberg (2009).

begs for caution when assessing ENSO simulations. Multiple centuries of simulation, and/or numerous ensemble members, may be required to robustly detect and attribute changes in ENSO arising from differing model formulations or changes in external forcings (C. Chen et al., 2017; Newman et al., 2018; Maher et al., 2018). The long timescales of ENSO modulation also suggest that existing instrumental records might not yet be sufficient to falsify some climate models, which motivates the use of paleoclimate proxies to help extend climate records deeper into the past (Vecchi & Wittenberg, 2010).

Intrinsic ENSO modulation can also imprint onto variability at decadal timescales, both through nonlinear rectification and by temporally "blurring" the interannual undulations of climatological features like the oceanic thermocline and atmospheric convergence zones (Vimont, 2005; Di Lorenzo et al., 2010; Wittenberg, 2015). A wood-working analogy for the temporal blurring effect would be switching on a power-sander: the tool's rapid oscillations *appear* to blur its edges into gradual visual transitions, even though the actual edges remain sharp at any given instant. As a result of this effect, model control simulations (Watanabe & Wittenberg, 2012; Watanabe et al., 2012; Ogata et al., 2013; Atwood et al., 2017) have shown that compared to weak-ENSO epochs, strong-ENSO epochs are associated with warmer time-mean SSTs in the far east Pacific, cooler time-mean SSTs at the eastern edge of the warm pool, intensified time-mean rainfall in the eastern equatorial Pacific, and a more diffuse ("blurred") time-mean vertical structure of the ocean thermocline. This can be seen in Figure 8.3, where relative to the weak-ENSO epoch (M5) the strong-ENSO epoch (M7) shows a clear warming of the multidecadal mean SST in the eastern equatorial Pacific.

Using a linearized version of the CZ model fit to the GFDL CM2.1 long control run of Figure 8.3, Atwood et al. (2017) concluded that the ENSO-induced multidecadal changes in time-mean ocean climate, in particular the climatological SST, surface winds, thermal stratification, currents, and upwelling, actually acted to *damp* the simulated ENSO during active-ENSO epochs, suggesting that the decadal ocean changes were a *symptom* rather than a cause of the amplified ENSO. However, CM2.1's active-ENSO epochs also tended to be linked to stronger and more zonally extensive stochastic wind forcing, and a more nonlinear wind stress response to SST anomalies (SSTA). This suggests that atmospheric nonlinearity, which was neglected from the intermediate model of Atwood et al. (2017), may be essential to maintaining the strong ENSO modulation in CM2.1. These results are consistent with the idea that both individual ENSO events and active-ENSO decades can be generated at random, by tropical Pacific wind stress noise and its nonlinear dependence on SST in the western/central

equatorial Pacific (Vecchi et al., 2006; Gebbie et al., 2007; Zavala-Garay et al., 2008, K.-Y. Choi et al., 2013, Fedorov et al., 2015, Capotondi et al., 2018).

On the other hand, Borlace et al. (2013) argued that in their 1000-year run using CSIRO Mk3L, the generated multidecadal ENSO modulations emerged as a result of gradual modulations of the tropical mean state in the model that modulated the strength of the thermocline feedback in the climate model, as assessed from the Bjerknes stability index (Jin et al., 2006); the effect on ENSO of mean state changes is discussed in more detail in the next subsection.

Atwood et al. (2017) further found that for the CM2.1 model, ENSO SST variance is roughly chi-square distributed, consistent with the hypothesis that the ENSO amplitude in one epoch is unrelated to that in its neighboring epochs. This may also explain why models with strong ENSO activity also tend to exhibit strong interdecadal modulation of ENSO amplitude (J. Choi et al., 2013; C. Chen et al., 2017): essentially, strong-ENSO models can generate both weak and strong epochs, while weak-ENSO models can only generate weak epochs. This motivates using amplitude modulation *relative* to the long-term average ENSO amplitude when comparing different simulations, evaluating models against observations, or assessing the impacts of external forcings.

Despite these results, a key question remains: Are the intrinsically generated modulations of ENSO in GCMs, seen for example in Figure 8.3, driven by the same processes as those seen in the observations (Figure 8.1), or are they an artifact of too strong an amplitude of the simulated ENSO, perhaps associated with the dominant internal mode being too unstable?

8.3. EXTERNALLY DRIVEN MODULATION OF ENSO

8.3.1. The Role of Tropical Pacific Mean State Changes

In contrast to the internally generated ENSO modulations that arise solely within the tropical ocean-atmosphere system due to intrinsic physics of El Niño and La Niña and potentially atmospheric noise, externally driven modulations require a mechanism or forcing different from ENSO. This "external" forcing should generate changes in the tropical Pacific on timescales longer than the ENSO characteristic timescales and can be due to a number of climate phenomena (e.g. the Pacific Decadal Oscillation, decadal variations in the Pacific Meridional Modes, the effects of other ocean basins on the tropical Pacific, changes caused by rising concentrations of atmospheric CO_2, etc.). Such a forcing modifies the mean state of the tropical Pacific on decadal and longer timescales, which in turn can give rise to low-frequency ENSO modulation.

That changes in the mean (or background) state of the tropical Pacific ocean-atmosphere system can affect ENSO has been known from the first studies of ENSO using the Cane-Zebiak model (1987) and its subsequent versions (Battisti & Hirst, 1989; Jin & Neelin, 1993; Fedorov & Philander, 2000, 2001; Chen & Cane, 2008). Several parameters characterizing the mean tropical state emerged as the key factors controlling ENSO characteristics, such as its amplitude, period, the structure and direction of propagation of SSTA, or the structure of precipitation anomalies. Among the most important are mean zonal winds, mean thermocline depth, ocean vertical stratification, or meridional temperature contrast across the equator, as was demonstrated by a stability analysis examining the eigenmodes of the tropical ocean-atmosphere system within models similar to the CZ model (Fedorov & Philander, 2000, 2001), see Figure 8.4,

and other studies (An & Jin, 2000; Wittenberg, 2002; Guilyardi, 2006; Collins et al., 2010).

How do changes in those characteristics of the tropical mean state affect ENSO? They do it by altering major feedbacks that control the period and the growth rates of the weakly damped or marginally unstable modes that give rise to ENSO. To understand their effects, one can consider the linearized equation for temperature rate of change written either for the ocean surface or mixed layer:

$$T_t^{'} = -\bar{u}T_x{'} - u'\bar{T}_x - \bar{v}T_y{'} - v'\bar{T}_y - \bar{w}T_z{'} - w'\bar{T}_z - Q' \quad (8.1)$$

Here, T is temperature; x and y are horizontal coordinates (corresponding to longitude and latitude respectively), z is ocean depth, and u, v, and w are velocity
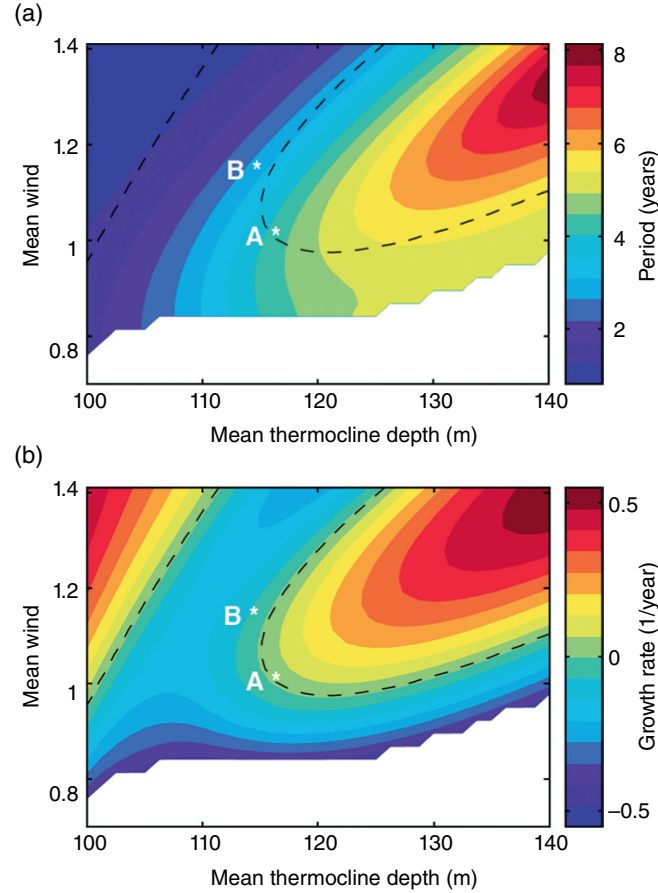

Figure 8.4 (a) The period (in years) and (b) growth rates (in 1/year) of the least damped/most unstable ENSO mode in an intermediate coupled model as a function of thermocline depth (in meters) along the horizontal axis and the intensity of easterly equatorial wind stress. Wind stress is given in nondimensional units such that 1 roughly corresponds to mean wind stress in the 1990s. Dashed lines indicate zero growth rate or neutral stability; there are no ENSO-like modes within the stable white area. Transitions from point B to A and then from A back to B would imply changes in ENSO similar to those that occurred in the late 1970s and then in the early 2000s. After Fedorov and Philander (2000, 2001).

components corresponding to those coordinates; t is time, subscripts indicate derivatives; bars and primes indicate mean and anomalous values, respectively. The terms on the right-hand-side of this equation describe various advective terms, except for the last one, which describes net atmospheric damping of temperature anomalies by surface heat fluxes.

Each of the advective/upwelling terms incorporates a particular feedback affecting ENSO. For example, $\bar{w}T_z'$ describes mean upwelling of anomalous temperature and contains the thermocline feedback, while $w'\bar{T}_z$ describes anomalous upwelling of mean temperature and hence contains the so-called Ekman feedback. The thermocline feedback is critical for ENSO as it communicates thermocline information to the ocean surface, making possible a dynamical coupling between the ocean and the atmosphere. It also largely controls the period of ENSO being close to 3–5 years. The Ekman feedback is weaker but can still be important in many models. Other terms of the equation, $\bar{u}T_x'$ and $u'\bar{T}_x$, $\bar{v}T_y'$ and $v'\bar{T}_y$, contain zonal and meridional advection feedbacks and also affect ENSO. At the same time, many of these terms, and Q', have components associated with damping of SST anomalies. Note that nonlinear terms neglected in Eq. 8.1 can also play an important role during strong El Niño events.

All of the aforementioned feedbacks are affected by changes in background conditions. In a linear framework, for example, the mean deepening of the thermocline or the strengthening of thermocline stratification might favor the thermocline feedback and produce longer periods and a stronger ENSO (e.g. Fedorov & Philander, 2000, 2001; Zhao & Fedorov, 2020). However, the relationship between particular changes in the mean state and ENSO is not straightforward because (i) the stability characteristics of the dominant ENSO mode(s) can vary nonmonotonically; (ii) mean state changes could simultaneously affect different feedbacks, damping effects, and possible nonlinearities; and (iii) changes in different characteristics of the mean state typically occur in parallel.

Actual changes in the mean thermocline depth and stratification are difficult to diagnose confidently, especially before the 1990s, given large variations due to ENSO and the sparsity of subsurface data; however, changes in mean winds appear to be measured more accurately for the past 30–40 years since the introduction of the in-situ buoys and the satellite scatterometer wind data. These measurements suggest a gradual strengthening of the zonal winds, in particular in the central-western tropical Pacific (Figure 8.5a) over the past three decades, suggesting a strengthening of the Walker circulation (McGregor et al., 2014; Hu & Fedorov, 2018). Figure 8.5a also shows a multidecadal strengthening of cross-equatorial winds in the eastern Pacific, which is confirmed by in-situ, satellite, and atmospheric reanalysis

data (Hu & Fedorov, 2018). This gradual strengthening of meridional winds is unlikely to be caused by ENSO changes and contains signals forced both locally and from outside the tropical Pacific, possibly from the tropical North Atlantic.

According to earlier studies with intermediate models focusing on zonal winds, and more recent studies with comprehensive GCMs focusing on both zonal and meridional winds, such a wind strengthening should lead to weaker ENSO variability. Indeed, imposing the strengthening of zonal or cross-equatorial wind anomalies comparable to that observed during the past three decades within perturbation experiments using a comprehensive climate GCM, for example CESM (Hu & Fedorov, 2018; Zhao & Fedorov, 2020), weakens the ENSO cycle (Figure 8.5d,e), producing changes similar to the observed shift in El Niño characteristics after the year 2000: a transition to CP events, the suppression of the ITCZ meridional migrations, and a shift toward more westward propagation of SST anomalies.

Finally, it is important to note again that even though changes in the mean state can clearly cause ENSO modulations, modulations of the same magnitude can occur in the comprehensive models without any changes in the mean state (as discussed in section 2), and the question of how to distinguish inherently generated versus externally driven ENSO modulations remains unresolved.

8.3.2. The Role of Other Ocean Basins

How do the changes in the mean state of the tropical Pacific discussed in the previous subsection come about? One possibility, to be discussed in section 8.4, is by interacting with decadal/multidecadal modes of climate variability in the Pacific. Another possibility involves the influence on the Pacific of other oceans (also see chapter 11). Model experiments and long proxy analyses suggest that other ocean basins have the ability to impact ENSO statistics on multidecadal timescales. The remotely forced changes to the tropical Pacific typically come via an atmospheric bridge driving changes in the Walker circulation. From the 1980s to the early 2010s, the Walker circulation strengthened (McGregor et al., 2014). Recent work on Pacific decadal trends and variability has shown that warming SSTs in the tropical Atlantic force additional convection locally and anomalous subsidence in the eastern tropical Pacific. The anomalous subsidence in the tropical Pacific increases the trade wind strength and the SST gradient across equatorial Pacific, essentially enhancing the Walker circulation and increasing the thermocline slope (McGregor et al., 2014, Kang et al., 2014, Li et al., 2016).

A warmer tropical Indian Ocean also can enhance the Walker circulation by driving additional Indian Ocean
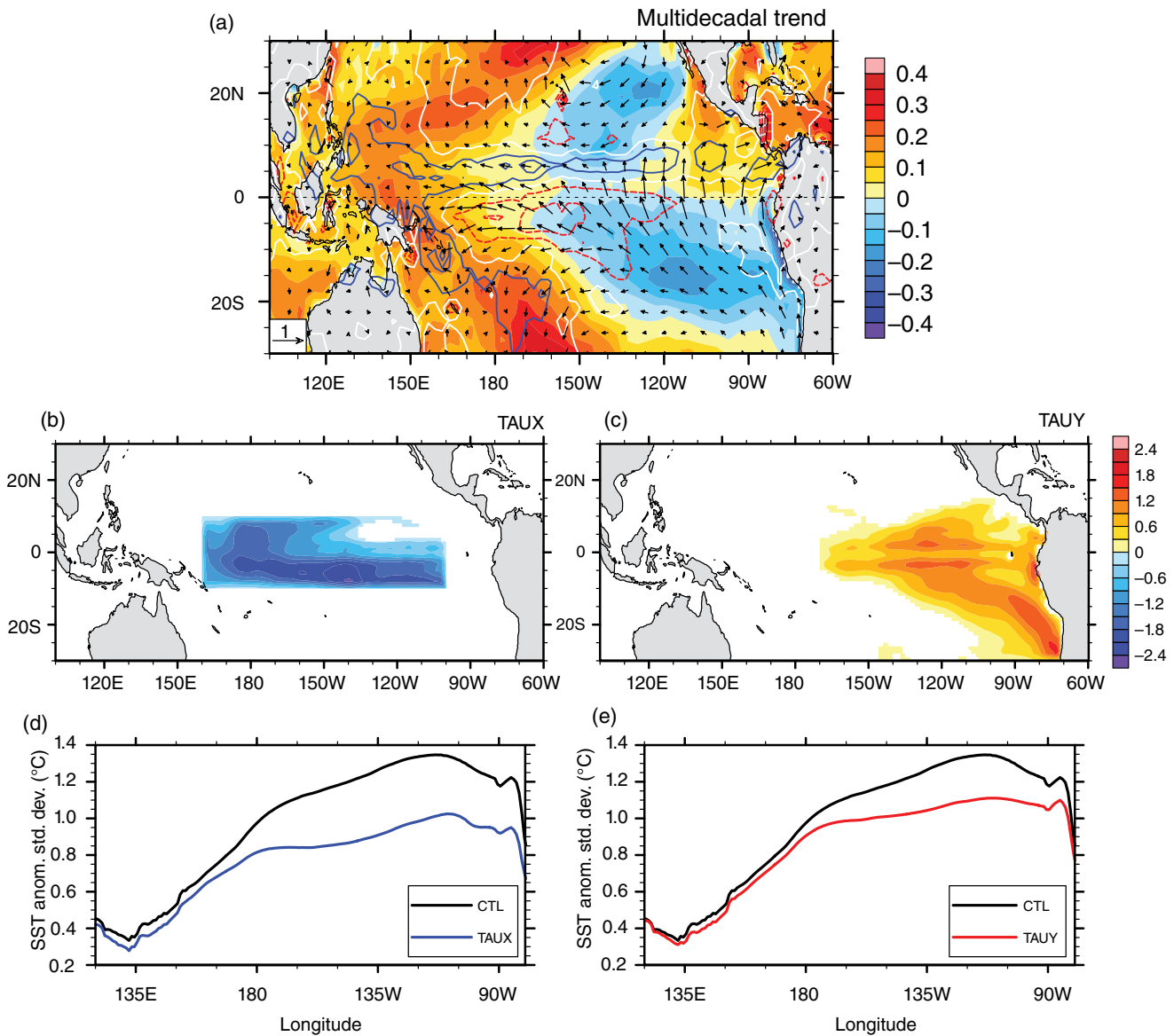
Figure 8.5 (a) Observed multidecadal trends in SST (colors; °C/decade), surface winds (vectors; m/s/decade), and precipitation (contours; 0.25 mm/day/decade interval) over the period of 1982–2015. For precipitation anomalies, blue, red, and white contours indicate positive, negative, and zero values, respectively. (b) Zonal and (c) meridional wind stress anomalies (10^{-2} N/m^2) superimposed in a coupled climate model (CESM) in the experiments named TAUX and TAUY, respectively. The magnitude of the superimposed wind stress anomalies is equivalent to three decades of the multidecadal trend during 1982–2015. (d,e) Standard deviations of equatorial (5°S–5°N) SST anomalies for (d) TAUX and (e) TAUY, in comparison with the control simulation (CTL). Note the reduction of ENSO variability in the eastern Pacific in both experiments. Panels a, c, and e are modified from Hu and Fedorov (2018).

convection and has also been suggested as a contributor to the changes in the tropical Pacific over the first decade and a half of the 21st century (Luo et al., 2012, Chikamoto et al., 2015, L. Dong & McPhaden, 2017b; Hu & Fedorov, 2019). Studies of the Indian Ocean forced trends in the Walker circulation implicate anthropogenic climate change (Luo et al., 2012; L. Dong & McPhaden, 2017b). Changes to the Walker circulation and upper ocean currents and stratification in the equatorial Pacific have been shown to change ENSO amplitude and frequency in models of intermediate complexity (Fedorov & Philander, 2000, 2001; Wittenberg, 2002; Bejarano & Jin, 2008).

But studies of the Atlantic are more mixed in cause. Previous model studies imposing a large cooling in the subpolar north Atlantic similar to the melting of the Greenland ice sheet lead to a decrease in ENSO amplitude and frequency (B. Dong et al., 2006, B. Dong & Sutton, 2007, Timmermann et al., 2007), while a recent study using an updated version of one of the same models found that changes in the noise forcing kept ENSO amplitude from changing noticeably, highlighting the challenge of distinguishing ENSO modulation from random fluctuation (Williamson et al., 2018).

More important in the context of the present-day climate is the effect on ENSO of natural SST variability in the Atlantic, known as the Atlantic multidecadal oscillation or variability (AMO or AMV; e.g. Enfield et al., 2001; Clement et al., 2015; R. Zhang et al., 2016). A combination of paleo and model evidence suggests that the changes in the north Atlantic SST due to the AMV could partially explain the multidecadal variability in ENSO through forced changes to the seasonal cycle of winds and currents in the equatorial Pacific (B. Dong et al., 2006, Zanchettin et al., 2016, Levine et al., 2017b, 2018, Hu & Fedorov, 2018). The changes in the seasonal cycle are strongly linked to changes in the ITCZ such as the strength and northward progression of the ITCZ during the boreal summer and fall (Levine et al., 2018). The AMV can also affect ENSO by inducing changes in the mean zonal and especially cross-equatorial winds in the Pacific (Hu & Fedorov, 2018). The latter study has shown that imposing a warming in the subtropical North Atlantic, a region strongly affected by the AMV, would induce a strong southerly cross-equatorial wind anomaly in the Pacific as well as a weak easterly wind anomaly, which would reduce ENSO amplitude and suppress the southward migration of the ITCZ, among other effects (Figure 8.6).

8.3.3. The Role of Model Biases

Another issue directly related to the effects of mean state changes on ENSO is the role of model climatological biases that affect their simulations of ENSO and hence the fidelity of ENSO decadal modulations simulated by coupled GCMs. These biases typically include a Pacific equatorial cold tongue (ECT) that is too intense and extends too far west (Burls et al., 2017; C. Chen et al., 2017; Thomas & Fedorov, 2017; Santoso et al., 2019). This ECT cold bias inhibits eastward and equatorward shifts of atmospheric deep convection during El Niño, leading to response patterns of rainfall, clouds, and westerly wind stress anomalies that are too weak and too far west (K.-Y. Choi et al., 2015; Ham & Kug, 2015; Capotondi et al., 2015b). This weakens both the wind stress *coupling* to SSTA, and the *damping* of

SSTA due to cloud shading in the equatorial Pacific, altering the balance of surface feedbacks during El Niño (Bellenger et al., 2014). It also reduces the positive (westerly) skewness of the equatorial wind stress response to SSTA, which contributes to the inability of most models to fully capture the observed amplitude, duration, and transition asymmetries between El Niño and La Niña (K.-Y. Choi et al., 2013), as well as the longer-term impacts of these ENSO asymmetries on decadal-scale variability (Lin et al., 2018).

A simulated ECT that extends too far west will also displace the region with large values of $\bar{T}_x$ (associated with the ECT/warm pool boundary) to the west. This westward displacement leads to excessive zonal separation of the SSTA induced by the zonal advective and thermocline feedbacks (related to the terms $-u'\bar{T}_x$ and $-\bar{w}T_z'$, respectively, in Eq. [8.1]), which then causes models to produce unrealistic "double-peaked" El Niño events (Graham et al., 2017). Models with stronger ECTs also tend to show excessive westward propagation of SSTA, due to an altered balance of subsurface advective feedbacks (Ham & Kug, 2015).

Biases in atmospheric processes can also directly influence ENSO's feedbacks. Most models still underestimate the meridional width of the equatorial westerly wind stress anomalies during El Niño, which hastens the discharge of equatorial subsurface heat content during warm events, weakens the events and accelerates their lifecycle, and shortens the ENSO period (Capotondi et al., 2006). Studies have shown that improving the atmosphere component's representation of the vertical transport of horizontal momentum by cumulus convection, through either enhanced atmospheric resolution or improved subgrid parameterizations, is one way to help broaden the meridional extent of the equatorial zonal wind stress anomalies and thereby lengthen and improve the simulated ENSO period (Kim et al., 2008; Neale et al., 2008).

Community efforts are underway to understand and address model climatological and ENSO biases in the tropical Pacific via improved ENSO diagnostics and metrics, enhanced model resolution, and better parameterization of subgridscale processes in the ocean and cloud physics in the atmosphere (Guilyardi et al., 2012a, 2016; Burls et al., 2017; also see chapter 9).

8.4. ENSO AND THE PACIFIC DECADAL OSCILLATION

As emphasized in the above discussion, changes in the mean state of the tropical Pacific can lead to ENSO modulation. On the other hand, the rectification of ENSO modulation can lead to the appearance of decadal variations in the tropical mean state. The major issue in
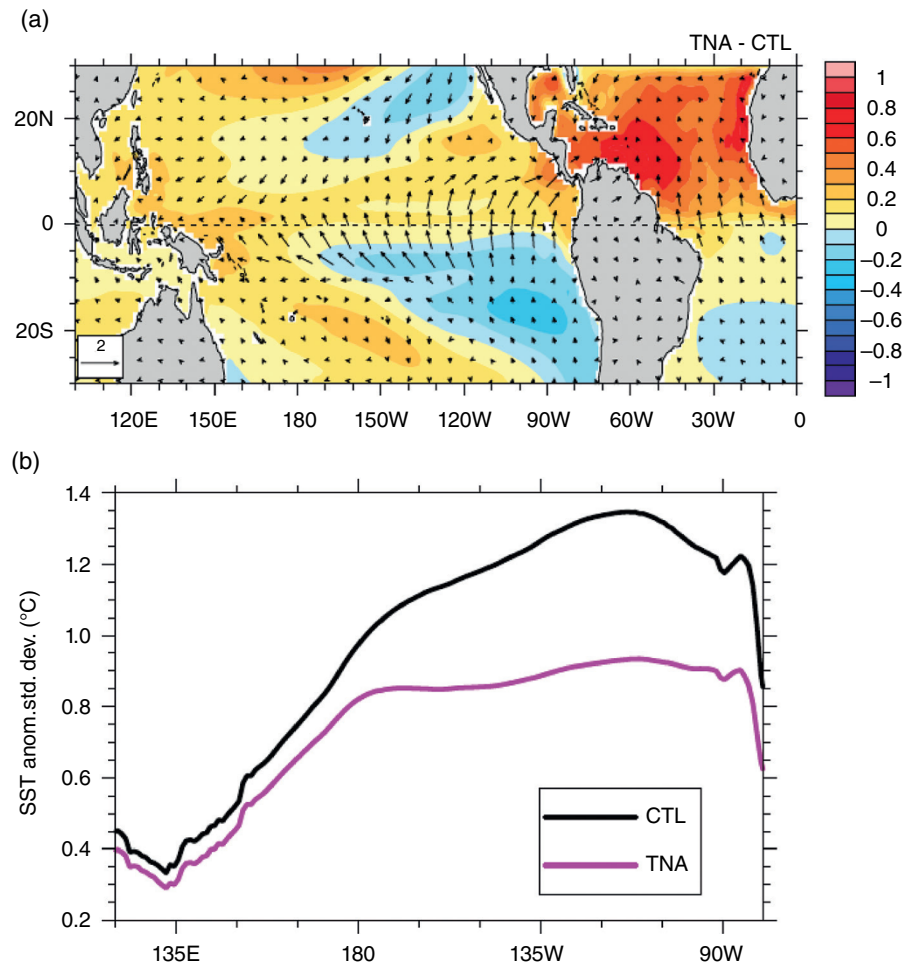
(a)

(b)

Figure 8.6 Tropical Atlantic warming as a cause for zonal and cross-equatorial wind strengthening in the Pacific and the subsequent changes in ENSO characteristics. (a) Anomalies in SST (colors; °C) and surface wind (vectors; m/s) in response to a tropical North Atlantic warming imposed between 0 and 30ºN in a coupled climate model (the simulation is called TNA). The imposed warming is constant in time but its magnitude (~0.5ºC) is equivalent to the observed trends over the past three decades. Note the simulated strengthening of mean zonal and meridional winds in the eastern Pacific. (b) Standard deviations of equatorial SST anomalies averaged within 5°S–5°N as a function of longitude for the control and TNA experiments. Note a significant reduction in the ENSO amplitude in the TNA experiment. The induced change in ENSO is very similar to that observed in the early 2000s (c.f. Figure 8.1d). After Hu and Fedorov (2018).

this context is the relationship between ENSO and the decadal/multidecadal modes of SST variability in the Pacific, and in particular its relationship with the dominant pattern of variability of monthly SSTA over the North Pacific (20–60°N) termed the "Pacific Decadal Oscillation" (PDO; Mantua et al., 1997; Figure 8.7). This basinwide structure, consisting of SSTA of one sign in the central and western North Pacific and the opposite sign along the eastern North Pacific, is linked to SSTA in the tropical and South Pacific, reminiscent of the pattern associated with the interannual ENSO phenomenon, albeit with weaker amplitude along the equator (Figure 8.7). This pan-Pacific structure is also known as

the "Interdecadal Pacific Oscillation" (IPO), defined as the leading mode of 13-year low-pass filtered Pacific SSTA after the secular global warming mode (Power et al., 1999).

The PDO/IPO is a coupled ocean-atmosphere phenomenon, as evidenced by its signature in surface winds (Figure 8.7). When the PDO/IPO is in its positive phase, the Aleutian low-pressure center is deeper than normal, accompanied by westerly wind anomalies over the central and western North Pacific and southerly wind anomalies in the eastern North Pacific.

Although it is convenient to describe the PDO/IPO as a single "mode" of variability with a unique spatial pattern

PDO

(a)

0.5 m/s

(b)

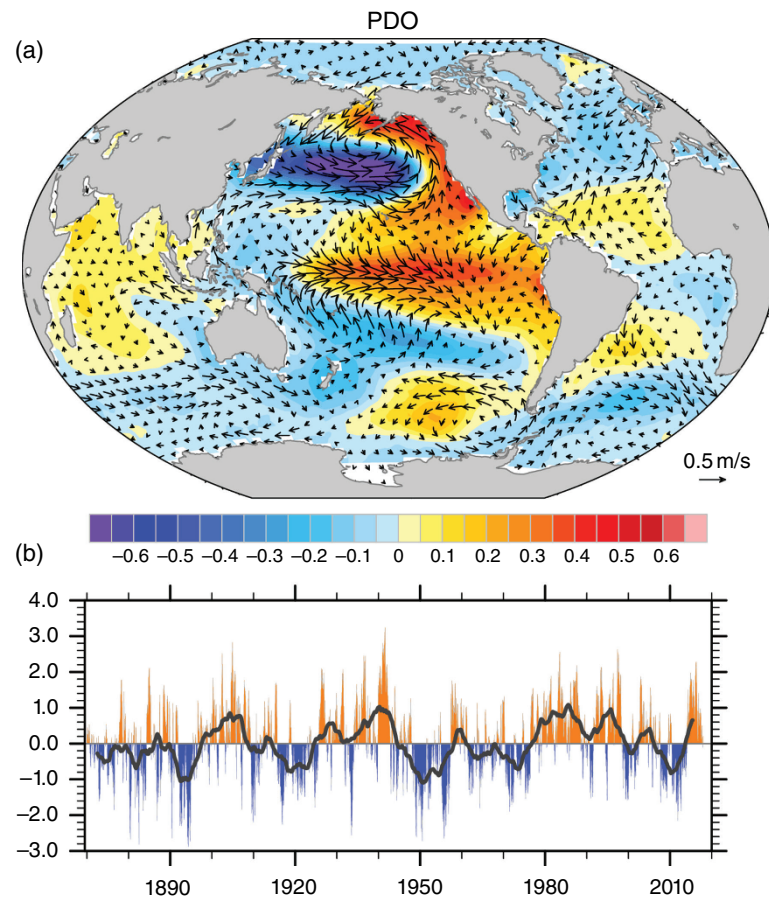-0.6 -0.5 -0.4 -0.3 -0.2 -0.1 0 0.1 0.2 0.3 0.4 0.5 0.6

Figure 8.7 Spatial pattern and temporal evolution of the PDO based on the ERSSTv5 SST data set during 1870–2017. The PDO is defined following Mantua et al. (1997) as the leading empirical orthogonal function and associated principal component (PC) time series based on monthly SSTA over the North Pacific (20°N–60°N) after subtracting the global mean SSTA. (a) Color shading shows global SSTA regressions (°C) and vectors show global surface wind anomaly regressions (ms⁻¹) upon the normalized PC time series. Winds are from the NOAA-CIRES 20th Century Reanalysis v2c. (b) PC time series. The heavy black line indicates a 61-month running mean.

and temporal history, it is now becoming apparent that a multitude of physical processes contribute to its characteristics (Newman et al., 2016). These include atmospheric teleconnections to the North and South Pacific driven by ENSO and their subsequent effects on the seasonal evolution of heat content anomalies in the upper ocean mixed layer (Vimont, 2005; Newman et al., 2003); stochastic atmospheric forcing of the North and South Pacific oceanic wind-driven gyre circulations via Rossby wave dynamics coupled with deterministic feedbacks of extratropical SSTA on to the atmosphere (Latif & Barnett, 1994; Deser et al., 1999; Schneider et al., 2002; Kwon & Deser, 2007; L. Zhang & Delworth, 2015); and the "seasonal footprinting mechanism," whereby SSTA in the North and South Pacific influence the tropical Pacific and the subsequent development of ENSO events (Vimont et al., 2001, 2003; DiLorenzo et al., 2008; Alexander et al., 2010). In view of this multiplicity of

processes, it is not surprising that the temporal and spatial characteristics of the PDO/IPO are challenging to define, understand, and predict. Indeed, alternate definitions of the PDO/IPO are being proposed based on distinguishing spatial patterns based on frequency characteristics (X. Chen & Wallace, 2016; Wills et al., 2018).

The observational record is too short to assess whether the temporal evolution of the PDO/IPO is truly oscillatory with a robust and statistically significant spectral peak, or simply part of a red noise continuum (Deser et al., 2004); it should be noted that the latter does not exclude "regime shift" behavior (Newman et al., 2016). Longer records of the PDO/IPO based on paleo-climate proxies are equivocal on this issue, with substantial disagreement among the different types of proxy records (Ault et al., 2013; Newman et al., 2016). For this reason, the term "Pacific decadal variability" is often used in place of PDO/IPO.

The ability of global coupled climate models to simulate the observed characteristics of the PDO/IPO varies greatly across models (Newman et al., 2016). In general, the models' PDO/IPO tends to have a higher autocorrelation and weaker linkages between the North and tropical Pacific compared to observations. In some long (millennial) control simulations without changes in external forcing, the PDO/IPO exhibits a distinct spectral peak at approximately 20 years that is statistically significant above a background red-noise continuum of variability (Deser et al., 2006; Kwon & Deser, 2007; L. Zhang & Delworth, 2015). This preferred timescale appears to arise from within the extratropical coupled ocean-atmosphere system, although interactions with the tropics can enhance the variability. Although the observed PDO/IPO time series exhibits a weak bidecadal spectral peak (Minobe, 1999; Deser et al., 2004), the most prominent timescale of variability is nominally 50 years (in a 118-year record; recall Figure 8.7), a timescale that models do not seem to capture. In one model, the PDO/IPO timescale has been shown to decrease from approximately 20 years to approximately 12 years in response to global warming, due to changes in ocean stratification and the phase speed of internal Rossby waves (L. Zhang & Delworth, 2016).

The frequency and amplitude of El Niño and La Niña events appear to be modulated by the phase of the PDO/IPO (Fedorov & Philander, 2000, 2001; An & Wang, 2000; Timmermann et al., 2003; Okumura et al., 2017; Lin et al., 2018) in both observations and models. This dependence can be explained by the sensitivity of ENSO dynamics to the mean state as described in section 8.3, in particular to changes in zonal winds evident in Figure 8.7. In fact, the wind and SST trends of the past several decades (Figure 8.5a) show a signature of the PDO/IPO negative phase together with a strong asymmetric component associated with cross-equatorial winds.

On the other hand, the connection between the frequency and amplitude of the ENSO cycle and the phase of the PDO/IPO could be related to the rectification of changes in ENSO on the mean state (Rodgers et al., 2004; Ogata et al., 2013; J. Choi et al., 2013; Wittenberg et al, 2014), which might imply a possibility of two-way interactions between ENSO and the PDO/IPO.

In addition to the PDO/IPO, other Pacific climate modes with a decadal component can give rise to ENSO modulations and ENSO/mean climate interactions. For example, the North Pacific Meridional Mode (Chiang & Vimont, 2004), driven by the coupling between tropical/subtropical meridional winds and SST variations, is known to modify zonal winds in the equatorial Pacific, thus linking the midlatitude North Pacific Oscillation to the tropics (Di Lorenzo et al., 2015).

8.5. ENSO DECADAL MODULATION IN OCEAN ENERGETICS

Recently, ocean energetics emerged as a powerful diagnostic tool for studying variability and ocean-atmosphere interactions in the tropical Pacific, including ENSO (Goddard & Philander, 2000; Fedorov, 2002; Fedorov et al., 2003; Fedorov, 2007; Brown & Fedorov, 2008, 2010; Brown et al., 2011; Hu et al., 2014; Kodama & Burls, 2019). Here, we discuss how ENSO decadal modulations are reflected in the energetics.

The ocean energetics describes the rate of change of the available potential energy (APE) induced by buoyancy power generated by the divergence of surface wind-driven currents; in turn, buoyancy power is closely related to the generated wind power. Mathematically, the balance of perturbation APE (or E for simplicity) can be represented as

$$\frac{dE}{dt} \approx \gamma W - \alpha E, \tag{8.2}$$

where W is perturbation wind power, γ is the efficiency of wind power conversion to the APE (50%–60%), and $-\alpha E$ represents APE damping (α is estimated in the range 0.5–1 year^{-1}), see Brown and Fedorov (2010) and Shi et al. (2020).

The perturbation E and W can be computed as follows:

$$E \approx \iiint \frac{\bar{\rho}\rho'}{S^2} dV, W \approx \iint \left(u'\overline{\tau} + \overline{u}\tau' \right) dA, \tag{8.3}$$

where ρ is potential density anomaly with respect to its time-mean horizontal average $\rho^*(z)$; $S^2 = -(1/g)d\rho^*(z)/dz$ describes mean vertical stratification in the tropical Pacific ocean; g is gravitational acceleration. Zonal ocean current velocity and surface wind stress are represented by u and τ, respectively; V and A are volume and surface area, respectively. Thus, E is computed as a weighted integral across the basin and with depth of density anomalies. In ENSO studies, this budget is typically considered for the tropical Pacific basin (15°S–15°N, 130°E–85°W). Vertical integration is conducted over the upper 400 m. Bars and primes describe the climatology and perturbation components; nonlinear terms in the expressions for E and W have been neglected.

Previous studies have shown that E describes changes in the equatorial thermocline slope and is well correlated with Niño3 anomalies on interannual timescales (Goddard & Philander, 2000; Brown & Fedorov, 2010). Typically, a positive (negative) E indicates a thermocline steeper (flatter) along the equator than the climatology. In accordance with Eq. 8.2, wind power leads E by 4–6 months with a correlation 0.6–0.7, providing an

alternative to ocean heat content as a precursor of El Niño (e.g. Kodama & Burls, 2019).

A recent study suggests that E could be used to characterize different types of El Niño events within the ENSO continuum; for example, higher negative E values correspond to EP events, and lower negative values to CP events (Hu et al., 2014). The same study also demonstrates that the ocean energetics framework is useful for understanding the impacts of intraseasonal wind bursts on the development, diversity, and predictability of El Niño events.

Ocean energetics also shed light on decadal variations in El Niño properties. The 1980s and 1990s witnessed strong El Niño activity, but after the year 2000 El Niño magnitude weakened (McPhaden et al., 2011; Hu & Fedorov, 2018; also see Figure 8.8a). Such decadal modulation of ENSO is especially striking in the variations of tropical Pacific APE (Figure 8.8b). During the 1980s and 1990s all El Niño events exhibit large negative values of E, but it is not so for warm events after 2000. That leads to a clear decadal shift in APE, even more pronounced than that in Niño3, which suggests that the decadal shift of El Niño properties involved much weaker subsurface thermocline variations and a reduced thermocline feedback.

Since direct calculations of E require ocean subsurface information, an alternative way to estimate E is to use sea surface height (SSH) information, as there is a tight connection between thermocline depth and SSH in the tropical Pacific (Shi et al., 2020). Accordingly, one can introduce an SSH index such that

$$E \propto SSH\,index = \iint \bar{h}h'dA, \qquad (8.4)$$

where h is SSH and the integral covers the same area of the tropical Pacific basin. Indeed, we find that this SSH index correlates with E extremely well (r = 0.95), both on interannual and decadal timescales (Figure 8.8c), although available satellite SSH measurements are relatively short.

These results suggest that the ocean energetics framework can be useful for understanding ENSO decadal modulations and potentially its decadal predictability. Do the correlations and lag between W and E change on decadal timescales? Does the efficiency γ change on decadal timescales? These questions will require further research.

8.6. PREDICTION OF ENSO DECADAL MODULATION

When decades of unusual ENSO behavior are observed in nature or in models, it is tempting to try to attribute them to some deterministic cause, such as slow changes in the climatological background state that might alter ENSO stability. However, coupled GCM experiments indicate that there is a large intrinsic component of ENSO modulation that may be essentially unpredictable on decadal timescales, and this random ENSO modulation can actually drive decadal variations in the background state.

For example, Wittenberg et al. (2014) examined the predictability of epochs of extreme ENSO behavior in the GFDL CM2.1 preindustrial control run. Figure 8.9 highlights two of the extreme-ENSO epochs from in Figure 8.3: the weak epoch M5 in Figure 8.9a, and the strong epoch M7 in Figure 8.9d. These two epochs display stark differences in their spatiotemporal behavior. The weak M5 epoch shows biennial SSTA variations, with westward SSTA propagation and near symmetry of the amplitude and pattern of warm and cold events. In contrast, the strong M7 epoch shows two distinct timescales (a quasi-biennial warm-to-cold transition, and a quasi-quadrennial interval between major warm events), with eastward SSTA propagation during warm events, and strong asymmetries between warm and cold events. Warm events here are shorter, more extreme, farther east, and more synchronized to the end of the calendar year than cold events, and warm-to-cold transitions are more robust than cold-to-warm transitions. These ENSO asymmetries in models and in nature have been attributed to the asymmetric wind stress response to SSTA, associated with the large equatorward and eastward shifts of atmospheric convection during strong El Niño events (Lengaigne et al., 2006; K.-Y. Choi et al., 2013, 2015).

Wittenberg et al. (2014) used a "perfect-model" approach, in which the model itself was used to "reforecast" its own previously generated trajectories. Before and during each extreme-ENSO epoch, the model trajectory was perturbed very slightly (adding 0.0001 K to a single ocean temperature cell), yielding an ensemble of 40 slightly perturbed members. The perturbed ensemble was then allowed to evolve forward in time according to the model dynamics.

Figure 8.9b shows that the weakest ENSO member from each of the three 40-member reforecasts does qualitatively reproduce the character of the weak M5 epoch. However, Figure 8.9c shows that the strongest ENSO member looks completely different, much more like the strong M7 epoch in Figure 8.8d. Thus, a mere flap of butterfly wings can cause an otherwise quiet ENSO epoch to explode into strong variability. Similarly, the weakest ENSO member from the M7 reforecasts (Figure 8.9e) demonstrates that butterflies can completely tame a strong-ENSO epoch. Wittenberg et al. (2014) found that the initially tiny perturbations grew rapidly over the first few years, inevitably leading to a complete loss of ENSO
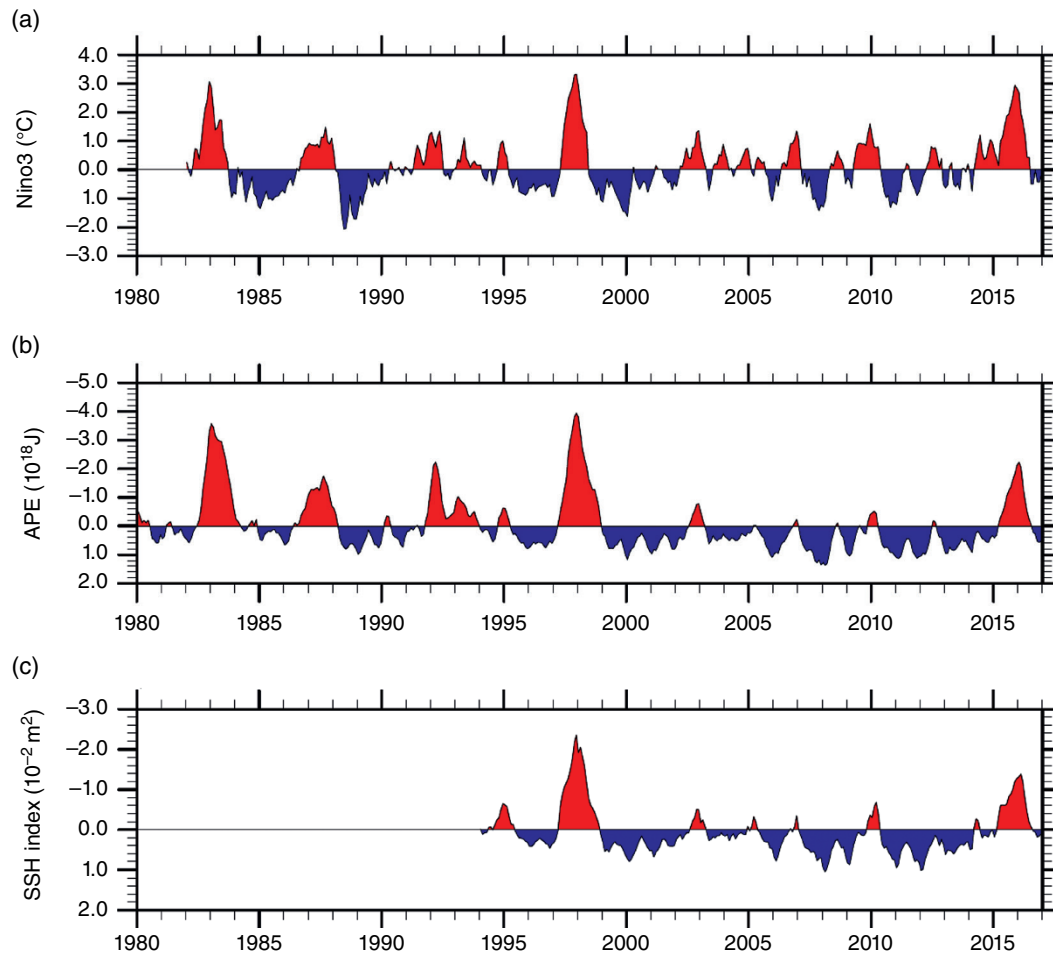
Figure 8.8 Variations in (a) Niño3 index, (b) perturbation available potential energy (*E*), and (c) SSH index. *E* and SSH index are defined in Eqs. (8.3) and (8.4). *E* is computed using the SODA ocean reanalysis. The vertical axes in (b) and (c) are reversed to facilitate comparison with the top panel. Note that decadal modulations of ENSO, including the shift after the year 2000, are especially pronounced in the energetics. After Shi et al. (2020).

predictability on decadal scales. Beyond about 3 years (roughly one ENSO cycle), the perturbed ensemble's ENSO amplitude became statistically indistinguishable from randomly selected states from the control run.

The results of Wittenberg et al. (2014) lend support to the hypothesis that interdecadal modulation of ENSO can arise even without variations in the ENSO's underlying dynamics (Newman et al., 2011a, 2011b). Realistically strong ENSO modulation is also found in simplified ENSO models that explicitly omit interactions with other basins or with external climate modes (see section 8.2.1). Just as flipping a fair coin will occasionally give an extended run of heads, an interannual ENSO with no decadal memory, i.e. a Poisson process with an interannual timescale, can occasionally produce multi-decadal quiet or active epochs (Wittenberg, 2009).

Figure 8.9 also illustrates how the unpredictable intrinsic component of ENSO modulation can impact the multidecadal mean state of the equatorial Pacific. The strong reforecast of the weak epoch (Figure 8.9c) shows warmer time-mean SST in the east and cooler SST in the west, associated with the asymmetry of ENSO amplitude and pattern between warm and cold events. The weak reforecast of the strong epoch (Figure 8.9e) shows the opposite, with multidecadal cooling of the east relative to the west. The key point is that substantial multidecadal changes in ENSO and the background climate can arise at random, and thus must be considered when attempting to attribute apparent changes to external radiative forcings or intermodel differences (section 8.3).

Even if the intrinsic component of ENSO modulation does turn out to be unpredictable on decadal scales, there still appears to be untapped potential for improved long-range ENSO forecasts at interannual scales. Ding et al. (2018, 2019) find that many coupled GCM simulations are now sufficiently realistic that their long control runs

Perfect-model reforecasts of extreme ENSO epochs.
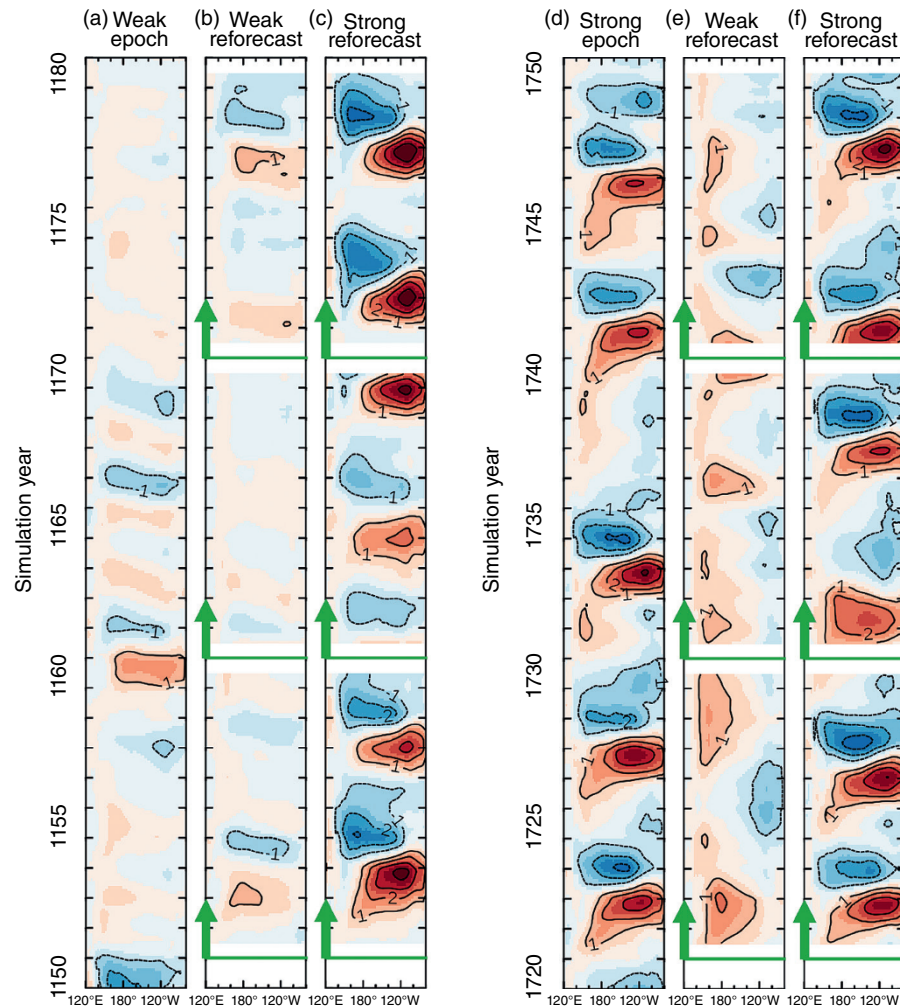SST anomalies (averaged 5°S–5°N), running annual mean.

Figure 8.9 Perfect-model reforecasts (Wittenberg et al., 2014) of two 30-year extreme-ENSO epochs from the multimillennium GFDL-CM2.1 coupled GCM preindustrial control run (Wittenberg, 2009). (a) Longitude-time plot of equatorial Pacific SSTA (averaged 5°S–5°N, running annual mean minus a 20-year low-pass climatology) during one of the weakest ENSO epochs in the control run (M5 in Figure 8.3). (b) The weakest ENSO trajectory from 40 perturbed reforecasts of the control run's weak-ENSO epoch, initialized at each of the three horizontal green lines and integrated forward in time for 10 years; the 20-year low-pass control-run climatology of (a) is subtracted, to highlight both the decadal and ENSO changes. (c) As in (b) but for the strongest ENSO trajectory from the 40 perturbed reforecasts. (d,e,f) As in (a,b,c) but for one of the strongest ENSO epochs in the control run (M7 in Figure 8.3); the 20-year low-pass control-run climatology from (d) is subtracted from each of (d,e,f). Contour interval is 1K, with shading incremented every half-contour. The zero contour is omitted for clarity.

can be used as "libraries" of analogs of real-world conditions. The time evolution of these "model-analogs" can then be used as actual forecasts, which exhibit real-world skill that actually outperforms state-of-the-art multimodel forecasts (initialized via comprehensive data assimilation) for the equatorial Pacific region. These fascinating results point to an exciting future where existing simulations could be used both to provide skillful and rapid ENSO forecasts and to reliably assess and attribute decadal-scale variations in ENSO's behavior and predictability.

8.7. ENSO MODULATION AND THE GLOBAL WARMING HIATUS

As is clear from the previous discussion, ENSO decadal modulation typically manifests as decades of particularly strong El Niño events (e.g. the 1980s and 1990s) alternat-

ing with decades of weak events (e.g. the 2000s). This becomes important in the context of the global warming "hiatus" of 1998–2013, a time interval when global mean surface temperature (GMST) remained steady, or at the very least the rate of GMST change was reduced (e.g., Trenberth & Fasullo, 2013; Trenberth et al., 2014; Schmidt et al., 2014; Fyfe et al., 2016). Similar "hiatus" intervals are seen throughout the climate record of the 20th century.

Several physical mechanisms have been offered to explain the most recent hiatus as well as other hiatuses, including but not limited to eastern Pacific cooling, Walker cell strengthening, enhanced ocean heat uptake, changes in stratospheric water vapor and aerosols, and atmospheric internal variability (e.g. Lyman et al., 2010; Solomon et al., 2010; Kaufmann et al., 2011; Levitus et al., 2012; Kosaka & Xie, 2013; Huber & Knutti, 2014; England et al., 2014; Santer et al., 2014; Schmidt et al., 2014; Watanabe et al., 2014; Dai et al., 2015; Liu et al., 2016; R. Zhang et al., 2016; L. Dong & McPhaden, 2017a; Deser et al. 2017a), while some argue that the hiatus itself depends on the datasets and the methods of analysis used (Karl et al., 2015).

Yet the simplest explanation for the hiatus comes from ENSO decadal modulation (Hu & Fedorov, 2017b). In fact, because of huge heat release from the ocean to the atmosphere, strong El Niño events have significant impacts on global mean temperatures, up to +0.2°C for such events as 1997 or 2015, which may last for a year or longer (Figure 8.10a). Strong La Niña events cool the planet, but the impacts are a little smaller. A sequence of strong and then weak El Niño events can easily create an appearance of a flat plateau in the GMST record, while a strong event such as El Niño of 2015 can give rise to a rapid warming. Consequently, ENSO decadal modulations lead to decadal modulations of GMST on the order of 1°C (Figure 8.10b).

A simple model that describes GMST and incorporates atmospheric heat release due to ENSO is given by the equation below (Hu & Fedorov, 2017b):

$$\frac{dT_g}{dt} = -\frac{T_g}{\tau} + a \cdot \log\left(\frac{CO_2}{CO_{2,ref}}\right) + b \cdot T_{NINO} + c \cdot SAOD + d, \text{ (8.5)}$$

where T_g is GMST, τ is a relaxation time scale, CO_2 and $CO_{2,ref}$ are carbon dioxide concentration and its reference level, T_{NINO} is SSTA averaged over the central-eastern equatorial Pacific, and $SAOD$ is stratospheric aerosol optical depth, which account for the impacts of volcanic eruptions. Using the best-fit model parameters a through d after training, this simple model reproduces the GMST history since the late 19th century very well (Figure 8.10c), including the global warming hiatus intervals. However, when the ENSO forcing is suppressed, the model fails to

capture not only interannual variations as expected, but also multidecadal variations, including the recent hiatus. Computations with comprehensive climate models with Niño3 temperature restored to the observed values also suggest the importance of ENSO modulations for GMST variations (Kosaka & Xie, 2013, 2014), although atmospheric internal variability and model biases in ENSO teleconnections must also be considered (Deser et al., 2017a).

8.8. CONCLUSIONS

Even though ENSO is the dominant climate mode on interannual timescales, it bridges a broad range of timescales, ranging from intraseasonal (westerly and easterly wind bursts, the Madden Julian oscillation) to multidecadal (the PDO/IPO, global warming trends). These different scales are not independent; for example, wind bursts are known to be modulated by ENSO (Eisenman et al., 2005; Yu et al., 2003) and possibly by decadal climate variability (Hu & Fedorov, 2016). On the other hand, a sequence of strong westerly wind bursts that occur during a favorable state of the tropical ocean-atmosphere, e.g. an enhanced ocean heat content, a warm pool extended to the east and/or reduced surface westward current (McPhaden & Yu, 1999; Hu et al., 2014; Fedorov et al., 2015; Hu & Fedorov, 2017a; Lengaigne et al., 2004; Thual et al., 2016), can lead to an extreme El Niño event or events, which may be sufficient to generate ENSO decadal modulation (Gebbie et al., 2007). In turn, such decadal modulations can affect global mean surface temperature and lead to either a transient rapid rise or hiatus in GMST. Yet global warming itself can modulate the properties of ENSO (chapter 13 in this book).

Overall, ENSO and tropical decadal variability are closely connected. For example, the weak ENSO activity since 2000, as compared to the 1980s and the 1990s, is suggested to be caused by the decadal strengthening of zonal and cross-equatorial winds in the eastern Pacific (e.g. Hu & Fedorov, 2018; Zhao & Fedorov, 2020). The zonal winds strengthen as part of the negative phase of the PDO, which should play a role in modulating ENSO properties, but the causality between the two phenomena is often hard to tease out (McPhaden et al., 2011; Capotondi et al., 2015a).

The question of causality remains one of the key questions of ENSO modulation as changes in the mean state affect the ENSO cycle, whereas ENSO modulation contributes to decadal variations. In fact, simple theories often treat PDO/IPO as a result of reddening of the ENSO signal (Newman et al., 2003) with additional dynamics in midlatitudes. Comparing the timeseries of the Niño3 SST (Figure 8.1a) and the PDO/IPO index (Figure 8.7b) one cannot help but notice that positive phases of the PDO/IPO correspond to the intervals of strong El Niño events while negative phases to weak El
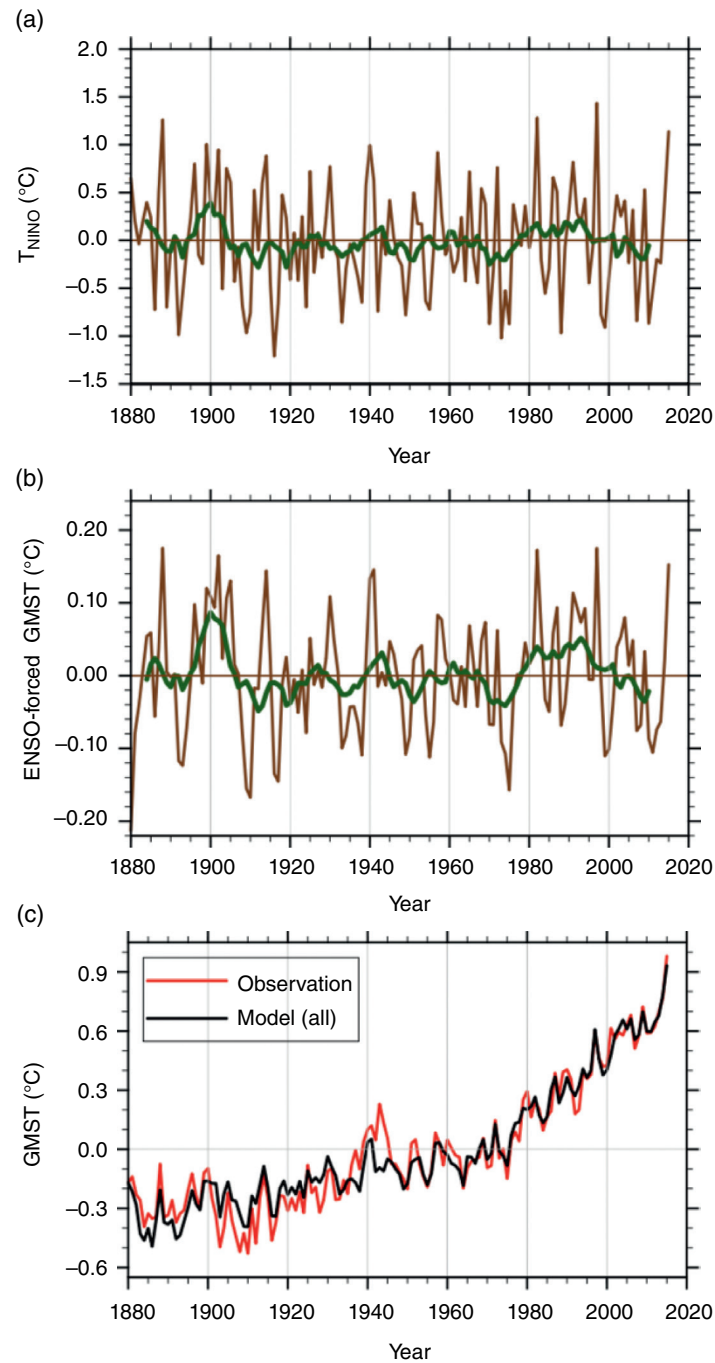
Figure 8.10 Modeled variations in (a) equatorial SST anomalies averaged within 5°S–5°N, 160°E–90°W ($T_{NIÑO}$) and (b) GMST when forced solely by this ENSO signal (i.e. Eq. [8.5] with CO_2 and volcanic forcing suppressed). Brown lines indicate annual means, while green lines indicate 10-year running means. Long-term means are removed from both variables. Note the modeled GMST has less power at higher frequencies. This reddening is a consequence of the system's thermal inertia. The ENSO forcing generates decadal variations in GMST with amplitude up to 0.1°C, which is sufficient to temporarily mask CO_2-induced trends of ~0.1°C per decade. (c) GMST variations estimated from the observations (red) and computed from the simple model (black) with all forcings in Eq. 8.5 active. After Hu and Fedorov (2017b).

Niño activity. Thus, a question arises: Is it the PDO/IPO modulating ENSO, or is it ENSO modulation that is responsible for the decadal variability?

Many other questions relevant to ENSO decadal modulations also remain unresolved. It was discovered early in computation with the Cane-Zebiak and other intermediate and hybrid coupled models that ENSO is very sensitive to small changes in various parameters such as the ocean-atmosphere coupling strength (e.g. Zebiak & Cane 1987; Battisiti & Hirst, 1989; Jin & Neelin, 1993; Fedorov & Philander, 2001; Wittenberg, 2002; Fedorov 2010) or the meridional extent of wind anomalies (Capotondi et al., 2006) or many different characteristics of the mean state as discussed in this chapter. It is now well recognized that ENSO can be extremely sensitive to the same parameters in complex GCMs and not necessarily in simple or intuitive ways. However, whether ENSO has the same sensitivity in nature is not clear. Likewise, it is not clear how unstable the internal mode describing ENSO is. GCMs that have a strongly unstable internal mode typically exhibit strong ENSO modulations without any external forcing, but also have an apparently excessive amplitude of El Niño.

Furthermore, how would one distinguish between the two main paradigms explaining the observed modulation of ENSO, i.e. internally generated variations due to the chaotic nature of the tropical coupled system versus externally driven variations due to forced changes in the tropical background state? This is a fundamental issue that might remain unresolved for some time. While it can be possible to answer this question in a particular climate GCM, even though the question of causality may be nontrivial, it is a much more difficult task to determine the answer in nature, especially given the limited length and accuracy of the available observations (~150 years). Just to obtain a statistically robust ENSO spectrum, one may have to run a GCM for 500 years or longer (e.g. Wittenberg, 2009). It is feasible that both paradigms operate at the same time: in models, inherently generated ENSO modulations are typically comparable in magnitude to ENSO changes caused by realistic changes in the mean state.

As models continue to improve, we may be able to more clearly distinguish the roles of external forcing from internal ENSO modulation. Also important are improved observations – including instrumental measurements to constrain the processes and feedbacks operating in simulations, paleo proxy records to illuminate the past behavior of ENSO, and comprehensive multicentury reanalyses to integrate all the diverse observations. Recent advances in those areas are described throughout this book and offer hope for better predictions and projections of ENSO and its modulation in the future. The most urgent question that we may be able to answer relatively soon is whether global warming is already affecting ENSO (chapter 13), as climate change represents perhaps the strongest perturbation experiment we can observe.

REFERENCES

Alexander, M. A., Vimont, D. J., Chang, P., & Scott, J. D. (2010). The impact of extratropical atmospheric variability on ENSO: Testing the seasonal footprinting mechanism using coupled model experiments. *Journal of Climate*, *23*(11), 2885–2901.

An, S.-I., & Jin, F.-F. (2000). An eigen analysis of the interdecadal changes in the structure and frequency of ENSO mode. *Geophys. Res. Lett.*, *27*, 2573–2576.

An, S. I., & Wang, B. (2000). Interdecadal change of the structure of the ENSO mode and its impact on the ENSO frequency. *Journal of Climate*, *13*(12), 2044–2055.

Ashok, K., Behera, S. K., Rao, S. A., Weng, H., & Yamagata, T. (2007). El Niño Modoki and its possible teleconnection. *Journal of Geophysical Research: Oceans*, *112*(C11).

Atwood, A. R., Battisti, D. S., Wittenberg, A. T., Roberts, W.G.H., & Vimont, D. J. (2017). Characterizing unforced multi-decadal variability of ENSO: A case study with the GFDL CM2.1 coupled GCM. Climate Dyn., 49 (7–8), 2845–2862. doi: 10.1007/s00382-016-3477-9.

Ault, T. R., Deser, C., Newman, M., & Emile-Geay, J. (2013). Characterizing decadal to centennial variability in the equatorial Pacific during the last millennium. *Geophysical Research Letters*, *40*(13), 3450–3456.

Battisti, D. S., & Hirst, A. C. (1989). Interannual variability in a tropical atmosphere–ocean model: Influence of the basic state, ocean geometry and nonlinearity. *Journal of the atmospheric sciences*, *46*(12), 1687–1712.

Bejarano, L., & Jin, F. F. (2008). Coexistence of equatorial coupled modes of ENSO. *Journal of Climate*, *21*(12), 3051–3067.

Bellenger, H., Guilyardi, E., Leloup, J., Lengaigne, J., & Vialard, J. (2014). ENSO representation in climate models: From CMIP3 to CMIP5. *Climate Dyn.*, *42*, 1999–2018. doi:10.1007/s00382-013-1783-z

Borlace, S., Cai, W., & Santoso, A. (2013). Multidecadal ENSO amplitude variability in a 1000-yr simulation of a coupled global climate model: Implications for observed ENSO variability. *J. Climate*, *26*, 9399–9407. doi:10.1175/JCLI-D-13-00281.1

Brown, J. N., & Fedorov, A. V. (2008). Mean energy balance in the tropical Pacific Ocean. *Journal of Marine Research*, *66*(1), 1–23.

Brown, J. N., & Fedorov, A. V. (2010). How much energy is transferred from the winds to the thermocline on ENSO time scales? *J Climate*, *23*(6), 1563–1580.

Brown, J. N., Fedorov, A. V., & Guilyardi, E. (2011). How well do coupled models replicate ocean energetics relevant to ENSO? *Clim Dynam*, *36*(11–12), 2147–2158.

Burgman, R. J., Schopf, P. S., & Kirtman, B. P. (2008). Decadal modulation of ENSO in a hybrid coupled model. *Journal of Climate*, *21*(21), 5482–5500.

Burls, N. J., Muir, L., Vincent, E. M., & Fedorov, A. (2017). Extra-tropical origin of equatorial Pacific cold bias in climate models with links to cloud albedo. *Climate Dynamics*, *49*(5–6), 2093–2113.

Cai, W., Borlace, S., Lengaigne, M., Van Rensch, P., Collins, M., Vecchi, G., et al. (2015). Increasing frequency of extreme El Niño events due to greenhouse warming. *Nature Climate Change*, *4*(2), 111.

Cane, M. A. (2005). The evolution of El Niño, past and future. *Earth and Planetary Science Letters*, *230*(3–4), 227–240.

Capotondi, A., & Sardeshmukh, P. D. (2017). Is El Niño really changing? *Geophysical Research Letters*, *44*(16), 8548–8556.

Capotondi, A., Wittenberg, A., & Masina, S. (2006). Spatial and temporal structure of tropical Pacific interannual variability in 20th century coupled simulations. *Ocean Modelling*, *15*, 274–298. doi: 10.1016/j.ocemod.2006.02.004

Capotondi, A., et al. (2015a). Understanding ENSO diversity. *Bull. Amer. Meteor. Soc.*, *96*, 921–938, doi:10.1175/BAMS-D-13-00117.1

Capotondi, A., Ham, Y.-G., Wittenberg, A. T., & Kug, J.-S. (2015b). Climate model biases and El Niño Southern Oscillation (ENSO) simulation. *U.S. CLIVAR Variations*, *13*(1), 21–25.

Capotondi, A., Sardeshmukh, P.D., & Ricciardulli, L. (2018). The nature of the stochastic wind forcing of ENSO. *J. Climate*, *31*(19) https://doi.org/10.1175/JCLI-D-17-0842.1

Chang, P., Wang, B., Li, T., & Ji, L. (1994). Interactions between the seasonal cycle and the Southern Oscillation-Frequency entrainment and chaos in a coupled ocean-atmosphere model. *Geophysical Research Letters*, *21*(25), 2817–2820.

Chen, D., & Cane, M. A. (2008). El Niño prediction and predictability. *Journal of Computational Physics*, *227*(7), 3625–3640.

Chen, C., Cane, M. A., Wittenberg, A. T., & Chen, D. (2017). ENSO in the CMIP5 simulations: Life cycles, diversity, and responses to climate change. *J. Climate*, *30* (2), 775–801. doi: 10.1175/JCLI-D-15-0901.1

Chen, D., Lian, T., Fu, C., Cane, M. A., Tang, Y., Murtugudde, R., et al. (2015). Strong influence of westerly wind bursts on El Niño diversity. *Nature Geoscience*, *8*(5), 339.

Chen, X., & Wallace, J. M. (2016). Orthogonal PDO and ENSO indices. *Journal of Climate*, *29*(10), 3883–3892.

Chiang, J. C., & Vimont, D. J. (2004). Analogous Pacific and Atlantic meridional modes of tropical atmosphere–ocean variability. *Journal of Climate*, *17*(21), 4143–4158.

Chikamoto, Y., Timmermann, A., Luo, J.-J., Mochizuki, T., Kimoto, M., Watanabe, M., et al. (2015). Skillful multi-year predictions of tropical trans-basin climate variability, *Nat. Commun.*, *6*, 6869.

Choi, J., An, S., Yeh, S., & Yu, J. (2013a). ENSO-Like and ENSO-Induced Tropical Pacific Decadal Variability in CGCMs. *J. Climate*, *26*, 1485–1501. doi: 10.1175/JCLI-D-12-00118.1

Choi, K.-Y., Vecchi, G. A., & Wittenberg, A. T. (2013b). ENSO transition, duration and amplitude asymmetries: Role of the nonlinear wind stress coupling in a conceptual model. *J. Climate*, *26*, 9462–9476. doi: 10.1175/JCLI-D-13-00045.1

Choi, K.-Y., Vecchi, G. A., & Wittenberg, A. T. (2015). Nonlinear zonal wind response to ENSO in the CMIP5 models: Roles of the zonal and meridional shift of the ITCZ/SPCZ and the simulated climatological precipitation. *J. Climate*, *28*, 8556–8573. doi: 10.1175/JCLI-D-15-0211.1

Clement, A., Bellomo, K., Murphy, L. N., Cane, M. A., Mauritsen, T., Rädel, G., & Stevens, B. (2015). The Atlantic Multidecadal Oscillation without a role for ocean circulation. *Science*, *350*(6258), 320–324.

Cobb, K. M., Charles, C. D., Cheng, H., & Edwards, R. L. (2003). El Niño/Southern Oscillation and tropical Pacific climate during the last millennium. *Nature*, *424*(6946), 271.

Cobb, K. M., Westphal, N., Sayani, H. R., Watson, J. T., Di Lorenzo, E., Cheng, H., et al. (2013). Highly variable El Niño–Southern Oscillation throughout the Holocene. *Science*, *339*(6115), 67–70.

Collins, M., An, S.-I., Cai, W., Ganachaud, A., Guilyardi, E., Jin, F.-F., et al. (2010). The impact of global warming on the tropical Pacific and El Niño. *Nature Geoscience*, *3*, 391–397. doi: 10.1038/ngeo868

Dai, A., Fyfe, J. C., Xie, S. P., & Dai, X. (2015). Decadal modulation of global surface temperature by internal climate variability. *Nat Clim Change*, *5*(6), 555–559.

Delworth, T. L., Broccoli, A. J., Rosati, A., Stouffer, R. J., Balaji, V., Beesley, J. A., et al. (2006). GFDL's CM2 global coupled climate models. Part I: Formulation and simulation characteristics. *Journal of Climate*, *19*(5), 643–674.

Deser, C., Alexander, M. A., & Timlin, M. S. (1999). Evidence for a wind-driven intensification of the Kuroshio Current Extension from the 1970s to the 1980s. *Journal of Climate*, *12*(6), 1697–1706.

Deser, C., Phillips, A. S., & Hurrell, J. W. (2004). Pacific interdecadal climate variability: Linkages between the tropics and the North Pacific during boreal winter since 1900. *Journal of Climate*, *17*(16), 3109–3124.

Deser, C., Capotondi, A., Saravanan, R., & Phillips, A. S. (2006). Tropical Pacific and Atlantic climate variability in CCSM3. *Journal of Climate*, *19*(11), 2451–2481.

Deser, C., Alexander, M. A., Xie, S. P., & Phillips, A. S. (2010). Sea surface temperature variability: Patterns and mechanisms. *Annual Review of Marine Science*, *2*, 115–143.

Deser, C., Phillips, A. S., Tomas, R. A., Okumura, Y., Alexander, M. A., Capotondi, A., et al. (2012). ENSO and Pacific Decadal Variability in Community Climate System Model Version 4. *J. Climate*, *25*, 2622–2651, 10.1175/JCLI-D-11-00301.1

Deser, C., Simpson, I. R., McKinnon, K. A., & Phillips, A. S. (2017a). The Northern Hemisphere extra-tropical atmospheric circulation response to ENSO: How well do we know it and how do we evaluate models accordingly? *J. Climate*, *30*, 5059–5082, doi: 10.1175/JCLI-D-16-0844.1

Deser, C., Guo, R., & Lehner, F. (2017b). The relative contributions of tropical Pacific sea surface temperatures and atmospheric internal variability to the recent global warming hiatus. *Geophysical Research Letters*, *44*(15), 7945–7954.

Di Lorenzo, E., Schneider, N., Cobb, K. M., Franks, P. J. S., Chhak, K., Miller, A. J., et al. (2008). North Pacific Gyre Oscillation links ocean climate and ecosystem change. *Geophysical Research Letters*, *35*(8).

Di Lorenzo, E., Cobb, K. M., Furtado, J. C., Schneider, N., Anderson, B. T., Bracco, A., et al. (2010). Central Pacific El Niño and decadal climate change in the North Pacific Ocean. *Nature Geosci.*, *3*, 762–765, doi:10.1038/ngeo984.

Di Lorenzo, E., Liguori, G., Schneider, N., Furtado, J. C., Anderson, B. T., & Alexander, M. A. (2015). ENSO and meridional modes: A null hypothesis for Pacific climate variability. *Geophysical Research Letters*, *42*(21), 9440–9448.

DiNezio, P. N., & Deser, C. (2014). Nonlinear controls on the persistence of La Niña. *Journal of Climate*, *27*(19), 7335–7355.

Ding, H., Newman, M., Alexander, M. A., & Wittenberg, A. T., (2018). Skillful climate forecasts of the tropical Indo-Pacific Ocean using model-analogs. *J. Climate*, *31*(14), 5437–5459. doi:10.1175/JCLI-D-17-0661.1

Ding, H., Newman, M., Alexander, M. A., & Wittenberg, A. T. (2019). Diagnosing secular variations in retrospective ENSO seasonal forecast skill using CMIP5 model-analogs. *Geophys. Res. Lett.*, *46* (3), 1721–1730. doi:10.1029/2018GL080598

Dong, B., & Sutton, R. T. (2007). Enhancement of ENSO variability by a weakened Atlantic thermohaline circulation in a coupled GCM. *J. Clim.*, *20*(19), 4920–4939.

Dong, B., Sutton, R. T., & Scaife, A. A. (2006). Multidecadal modulation of El Niño-Southern Oscillation (ENSO) variance by Atlantic Ocean sea surface temperatures. *Geophys. Res. Lett.*, *33*, L08705, doi:10.1029/2006GL025766.

Dong, L., & McPhaden, M. J. (2017a). The role of external forcing and internal variability in regulating global mean surface temperatures on decadal timescales, *Environ. Res. Lett.*, *12*(3), 034011.

Dong, L., & McPhaden, M. J. (2017b). Why has the relationship between Indian and Pacific Ocean decadal variability changed in recent decades? *J. Clim.*, *30*, 1971–1983.

Eisenman, I., Yu, L., & Tziperman, E. (2005). Westerly wind bursts: ENSO's tail rather than the dog? *Journal of Climate*, *18*(24), 5224–5238.

Enfield, D. B., Mestas-Nuñez, A. M., & Trimble, P. J. (2001). The Atlantic Multidecadal Oscillation and its relation to rainfall and river flows in the continental U.S. *Geophys. Res. Lett.*, *28*(10), 2077–2080.

England, M. H., McGregor, S., Spence, P., Meehl, G. A., Timmermann, A., Cai, W., et al. (2014). Recent intensification of wind-driven circulation in the Pacific and the ongoing warming hiatus. *Nature Climate Change*, *4*(3), 222.

Fedorov, A. V. (2002). The response of the coupled tropical ocean-atmosphere to westerly wind bursts, *Q J Roy Meteor Soc*, *128*(579), 1–23.

Fedorov, A. V. (2007). Net energy dissipation rates in the tropical ocean and ENSO dynamics, *J Climate*, *20*(6), 1108–1117.

Fedorov, A. V. (2010). Ocean response to wind variations, warm water volume, and simple models of ENSO in the low-frequency approximation. *Journal of Climate*, *23*(14), 3855–3873.

Fedorov, A. V., & Philander, S. G. (2000). Is El Niño changing? *Science*, *288*(5473), 1997–2002.

Fedorov, A. V., & Philander, S. G. (2001). A stability analysis of tropical ocean–atmosphere interactions: Bridging measurements and theory for El Niño. *J. Clim.*, *14*(14), 3086–3101.

Fedorov, A. V., Harper, S. L., Philander, S. G., Winter, B., & Wittenberg, A. (2003). How predictable is El Niño? *Bulletin of the American Meteorological Society*, *84*(7), 911–920.

Fedorov, A. V., Hu, S., Lengaigne, M., & Guilyardi, E. (2015). The impact of westerly wind bursts and ocean initial state on the development, and diversity of El Niño events. *Climate Dynamics*, *44*(5–6), 1381–1401.

Flügel, M., Chang, P., & Penland, C. (2004). The role of stochastic forcing in modulating ENSO predictability. *J. Climate*, *17*, 3125–3140.

Fyfe, J. C., et al. (2016). Making sense of the early-2000s warming slowdown. *Nat Clim Change*, *6*(3), 224–228.

Gebbie, G., Eisenman, I., Wittenberg, A., & Tziperman, E. (2007). Modulation of westerly wind bursts by sea surface temperature: A semistochastic feedback for ENSO. *J. Atmos. Sci.*, *64*, 3281–3295. doi: 10.1175/JAS4029.1

Goddard, L., & Philander, S. G. (2000). The energetics of El Niño and La Niña. *J Climate*, *13*(9), 1496–1516.

Graham, F. S., Wittenberg, A. T., Brown, J. N., Marsland, S. J., & Holbrook, N. J. (2017). Understanding the double peaked El Niño in coupled GCMs. *Climate Dyn.*, *48* (5), 2045–2063. doi: 10.1007/s00382-016-3189-1

Guilyardi, E. (2006). El Niño–mean state–seasonal cycle interactions in a multi-model ensemble. *Climate Dynamics*, *26*(4), 329–348.

Guilyardi, E., Wittenberg, A., Fedorov, A., Collins, M., Wang, C., Capotondi, A., et al. (2009). Understanding El Niño in ocean–atmosphere general circulation models: Progress and challenges. *Bulletin of the American Meteorological Society*, *90*(3), 325–340.

Guilyardi, E., Bellenger, H., Collins, M., Ferrett, S., Cai, W., & Wittenberg, A. (2012a). A first look at ENSO in CMIP5. *Clivar Exchanges*, *17*(1), 29–32.

Guilyardi, E., Cai, W., Collins, M., Fedorov, A., Jin, F. F., Kumar, A., et al. (2012b). New strategies for evaluating ENSO processes in climate models. *Bulletin of the American Meteorological Society*, *93*(2), 235–238.

Guilyardi, E., A. Wittenberg, M. Balmaseda, W. Cai, M. Collins, M. J. McPhaden, et al. (2016). Fourth CLIVAR Workshop on the Evaluation of ENSO Processes in Climate Models: ENSO in a Changing Climate. *Bull. Amer. Meteor. Soc.*, *97*(5), 817–820. doi: 10.1175/BAMS-D-15-00287.1

Hannachi, A., Stephenson, D. B., & Sperber, K. R. (2003). Probability-based methods for quantifying nonlinearity in the ENSO. *Clim. Dyn.*, *20*(2–3), 241–256.

Ham, Y., & Kug, J.-S. (2015). Improvement of ENSO simulation based on intermodel diversity. *J. Climate*, *28*, 998–1015. doi:10.1175/JCLI-D-14-00376.1

Harrison, D.E., & Chiodi, A.M. (2009). Pre- and post-1997/98 westerly wind events and equatorial Pacific cold tongue warming. *J. Climate*, *22*, 568–581, https://doi.org/10.1175/2008JCLI2270.1

Hu, S., & Fedorov, A. V. (2016) Exceptionally strong easterly wind burst stalling El Niño of 2014. *Proc. Natl. Acad. Sci. U.S.A.*, *113*(8), 2005–2010.

Hu, S., & Fedorov, A. V. (2017a). The extreme El Niño of 2015–2016: The role of westerly and easterly wind bursts, and preconditioning by the failed 2014 event. *Clim. Dynam. doi*: 10.1007/s00382-017-3531-2.

Hu, S., & Fedorov, A. V. (2017b). The extreme El Niño of 2015–2016 and the end of global warming hiatus. *Geophys. Res. Lett.*, *44*(8), 3816–3824.

Hu, S., & Fedorov, A. V. (2018). Cross-equatorial winds control El Niño diversity and change. *Nature Climate Change*, *8*(9), 798.

Hu, S., & Fedorov, A. V. (2019). Indian Ocean warming can strengthen the Atlantic meridional overturning circulation. *Nature Climate Change*, *9*(10), 747–751.

Hu, S., Fedorov, A. V., Lengaigne, M., & Guilyardi, E., (2014). The impact of westerly wind bursts on the diversity and predictability of El Niño events: An ocean energetics perspective. *Geophys. Res. Lett.*, *41*(13), 4654–4663.

Huber, M., & Knutti, R. (2014). Natural variability, radiative forcing and climate response in the recent hiatus reconciled. *Nat Geosci*, *7*(9), 651–656.

Jin, F.F. (1997). An equatorial ocean recharge paradigm for ENSO. Part I: Conceptual model. *Journal of the Atmospheric Sciences*, *54*(7), 811–829.

Jin, F. F., & Neelin, J. D. (1993). Modes of interannual tropical ocean–atmosphere interaction—A unified view. Part I: Numerical results. *Journal of the Atmospheric Sciences*, *50*(21), 3477–3503.

Jin, F.-F., Neelin, J. D., & Ghil, M. (1994). El Niño on the devil's staircase: Annual subharmonic steps to chaos. *Science*, *264*(5155), 70–72.

Jin, F. F., Neelin, J. D., & Ghil, M. (1996). El Nino/Southern Oscillation and the annual cycle: Subharmonic frequency-locking and aperiodicity. *Physica D: Nonlinear Phenomena*, *98*(2-4), 442–465.

Jin, F. F., An, S. I., Timmermann, A., & Zhao, J. (2003). Strong El Niño events and nonlinear dynamical heating. *Geophysical Research Letters*, *30*(3), 20–21.

Jin, F. F., Kim, S. T., & Bejarano, L. (2006). A coupled-stability index for ENSO. *Geophysical Research Letters*, *33*(23).

Kao, H. Y., & Yu, J. Y. (2009). Contrasting eastern-Pacific and central-Pacific types of ENSO. *Journal of Climate*, *22*(3), 615–632.

Kang, I.-S., No, H.-h., & Kucharski, F. (2014). ENSO amplitude modulation associated with the mean SST changes in the tropical central Pacific induced by Atlantic Multidecadal Oscillation. *J. Clim.*, *27*(20), 7911–7920.

Karamperidou, C., Cane, M. A., Lall, U., & Wittenberg, A. T. (2014). Intrinsic modulation of ENSO predictability viewed through a local Lyapunov lens. *Climate Dyn.*, *42*, 253–270. doi: 10.1007/s00382-013-1759-z

Karl, T. R., Arguez, A., Huang, B. Y., Lawrimore, J. H., McMahon, J. R., Menne, M. J., et al. (2015), Possible arti-facts of data biases in the recent global surface warming hiatus. *Science*, *348*(6242), 1469–1472.

Karspeck, A.R., Seager, R. & Cane, M.A. (2004). Predictability of tropical Pacific decadal variability in an intermediate model. *Journal of Climate*, *17*(14), 2842–2850.

Kaufmann, R. K., Kauppi, H., Mann, M. L., & Stock, J. H. (2011). Reconciling anthropogenic climate change with observed temperature 1998–2008. *Proc. Natl Acad. Sci. USA*, *108*, 11790–11793.

Kim, D., Kug, J.-S., Kang, I.-S., Jin, F.-F., & Wittenberg, A. T. (2008). Tropical Pacific impacts of convective momentum transport in the SNU coupled GCM. *Climate Dyn.*, *31*, 213–226. doi: 10.1007/s00382-007-0348-4

Kirtman, B. P., & Schopf, P. S. (1998). Decadal variability in ENSO predictability and prediction. *Journal of Climate*, *11*(11), 2804–2822.

Kodama, K., & Burls, N. (2019). An empirical adjusted ENSO ocean energetics framework based on observational wind power in the tropical Pacific. *Climate Dynamics*, *53*, 3271–3288.

Kosaka, Y., & Xie, S. P. (2013). Recent global-warming hiatus tied to equatorial Pacific surface cooling. *Nature*, *501*(7467), 403–407.

Kug, J. S., Jin, F. F., & An, S. I. (2009). Two types of El Niño events: Cold tongue El Niño and warm pool El Niño. *Journal of Climate*, *22*(6), 1499–1515.

Kug, J.-S., Choi J., An S.-I., Jin F.-F., & Wittenberg A. T. (2010). Warm pool and cold tongue El Niño events as simulated by the GFDL CM2.1 coupled GCM. *J. Climate*, *23*, 1226–1239. doi: 10.1175/2009JCLI3293.1

Kwon, Y. O., & Deser, C. (2007). North Pacific decadal variability in the community climate system model version 2. *Journal of Climate*, *20*(11), 2416–2433.

Latif, M., & Barnett, T. P. (1994). Causes of decadal climate variability over the North Pacific and North America. *Science*, *266*(5185), 634–637.

Lee, S. K., DiNezio, P. N., Chung, E. S., Yeh, S. W., Wittenberg, A. T., & Wang, C. (2014). Spring persistence, transition, and resurgence of El Niño. *Geophysical Research Letters*, *41*(23), 8578–8585.

Lee, S. K., Wittenberg, A. T., Enfield, D. B., Weaver, S. J., Wang, C., & Atlas, R. (2016). US regional tornado outbreaks and their links to spring ENSO phases and North Atlantic SST variability. *Environmental Research Letters*, *11*(4), 044008.

Lee, S. K., Lopez, H., Chung, E. S., DiNezio, P., Yeh, S. W., & Wittenberg, A. T. (2018). On the fragile relationship between El Niño and California rainfall. *Geophysical Research Letters*, *45*(2), 907–915.

Lengaigne, M., Guilyardi, E., Boulanger, J. P., Menkes, C., Delecluse, .P, Inness, P., et al.(2004). Triggering El Niño by westerly wind events in a coupled general circulation model. *Clim Dyn*, *23*, 601–620.

Lengaigne, M., Boulanger, J. P., Menkes, C., & Spencer, H. (2006). Influence of the seasonal cycle on the termination of El Niño events in a coupled general circulation model. *Journal of Climate*, *19*(9), 1850–1868.

Levine, A. F., & Jin, F. F., (2010). Noise-induced instability in the ENSO recharge oscillator. *Journal of the Atmospheric Sciences*, *67*(2), 529–542.

Levine, A. F., & McPhaden, M. J. (2016). How the July 2014 easterly wind burst gave the 2015–2016 El Niño a head start. *Geophysical Research Letters*, *43*(12), 6503–6510.

Levine, A., Jin, F. F., & McPhaden, M. J. (2016). Extreme noise–extreme El Niño: How state-dependent noise forcing creates El Niño–La Niña asymmetry. *Journal of Climate*, *29*(15), 5483–5499.

Levine, A. F. Z., Jin, F.-F., & Stueker, M. F. (2017a). A simple approach to quantifying the noise-ENSO interaction. *Part II: The role of coupling between the warm pool and equatorial zonal wind anomalies. Climate Dyn.*, *48*, 19–37.

Levine, A. F. Z., McPhaden, M. J., & Frierson, D. M. W. (2017b). The impact of the AMO on multidecadal ENSO variability. *Geophys. Res. Lett.*, *44*, doi:10.1002/2017GL072524

Levine, A. F., Frierson, D. M., & McPhaden, M. J. (2018). AMO forcing of multidecadal Pacific ITCZ variability. *Journal of Climate*, *31*(14).

Levitus, S., et al. (2012). World ocean heat content and thermosteric sea level change (0–2000 m), 1955–2010. *Geophys Res Lett*, *39*(10), L10603.

Li, X., Xie, S. P., Gille, S. T., & Yoo, C. (2016). Atlantic-induced pan-tropical climate change over the past three decades. *Nature Climate Change*, *6*(3), 275.

Lin, R., Zheng, F., & Dong, X., (2018). ENSO frequency asymmetry and the Pacific decadal oscillation in observations and 19 CMIP5 models. *Adv. Atmos. Sci.*, *35*, 495–506. doi:10.1007/s00376-017-7133-z

Liu, W., Xie, S.-P., & Lu, J. (2016). Tracking ocean heat uptake during the surface warming hiatus. *Nat. Commun.*, *7*, doi:10.1038/ncomms10926

Lorenz, E. N. (1963). Deterministic nonperiodic flow. *Journal of the Atmospheric Sciences*, *20*(2), 130–141.

Luo, J.-J., Sasaki, W., & Masumoto, Y. (2012). Indian Ocean warming modulates Pacific climate change. *Proc. Natl. Acad. Sci. U.S.A.*, *109*(46), 18,701–18,706.

Lyman, J. M., Good, S. A., Gouretski, V. V., Ishii, M., Johnson, G. C., Palmer, M. D., et al. (2010). Robust warming of the global upper ocean. *Nature*, *465*(7296), 334–337.

Maher, N., Matei, D., Milinski, S., & Marotzke, J. (2018). ENSO change in climate projections: Forced response or internal variability? *Geophys. Res. Lett.*, *45*, 11,390–11398.

Mantua, N. J., Hare, S. R., Zhang, Y., Wallace, J. M., & Francis, R. C. (1997). A Pacific interdecadal climate oscillation with impacts on salmon production. *Bulletin of the American Meteorological Society*, *78*(6), 1069–1080.

Manucharyan, G. E., & Fedorov, A. V. (2014). Robust ENSO across a wide range of climates. *Journal of Climate*, *27*(15), 5836–5850.

McGregor, S., Timmermann, A., England, M. H., Elison Timm, O., & Wittenberg, A. T. (2013). Inferred changes in El Niño-Southern Oscillation variance over the past six centuries. *Clim. Past*, *9*, 2269–2284. doi: 10.5194/cp-9-2269-2013.

McGregor, S., Timmermann, A., Stuecker, M. F., England, M. H., Merrifield, M., Jin, F.-F., & Chikamoto, Y. (2014). Recent Walker circulation strengthening and Pacific cooling amplified by Atlantic warming. *Nat. Clim. Change*, *4*(10), 888–892.

McPhaden, M. J., & Yu, X. (1999). Equatorial waves and the 1997–98 El Niño. *Geophysical Research Letters*, *26*(19), 2961–2964.

McPhaden, M. J., Lee, T., & McClurg, D. (2011). El Niño and its relationship to changing background conditions in the tropical Pacific Ocean. *Geophysical Research Letters*, *38*(15).

Meehl, G. A., Hu, A., & Santer, B. D. (2009). The mid-1970s climate shift in the Pacific and the relative roles of forced versus inherent decadal variability. *Journal of Climate*, *22*(3), 780–792.

Meinen, C. S., & McPhaden, M. J. (2000). Observations of warm water volume changes in the equatorial Pacific and their relationship to El Niño and La Niña. *Journal of Climate*, *13*(20), 3551–3559.

Minobe, S. (1999). Resonance in bidecadal and pentadecadal climate oscillations over the North Pacific: Role in climatic regime shifts. *Geophysical Research Letters*, *26*(7), 855–858.

Mu, M., Duan, W., & Wang, B. (2007). Season-dependent dynamics of nonlinear optimal error growth and El Niño-Southern Oscillation predictability in a theoretical model. *Journal of Geophysical Research: Atmospheres*, *112*(D10).

Neale, R. B., Richter J. H., & Jochum M., (2008). The impact of convection on ENSO: From a delayed oscillator to a series of events. *J. Climate*, *21*, 5904–5924. doi:10.1175/2008JCLI2244.1

Newman, M., Compo, G. P., & Alexander, M. A. (2003). ENSO-forced variability of the Pacific decadal oscillation. *Journal of Climate*, *16*(23), 3853–3857.

Newman, M., Alexander, M. A., & Scott, J. D., (2011a). An empirical model of tropical ocean dynamics. *Climate Dyn.*, *37*, 1823–1841. doi:10.1007/s00382-011-1034-0

Newman, M., Shin, S.-I., & Alexander, M. A., (2011b). Natural variation in ENSO flavors. *Geophys. Res. Lett.*, *38*, L14705, doi:10.1029/2011GL047658

Newman, M., Alexander, M. A., Ault, T. R., Cobb, K. M., Deser, C., Di Lorenzo, E., et al. (2016). The Pacific decadal oscillation, revisited. *Journal of Climate*, *29*(12), 4399–4427.

Newman, M., Wittenberg, A. T., Cheng, L., Compo, G. P., & Smith, C. A., (2018). The extreme 2015/16 El Niño, in the context of historical climate variability and change. Section 4 of: "Explaining extreme events of 2016 from a climate perspective." *Bull. Amer. Meteor. Soc.*, *99*(1), S16–S20. doi: 10.1175/BAMS-D-17-0116.1

Ogata, T., Xie, S.-P., Wittenberg, A., & Sun, D.-Z. (2013). Interdecadal amplitude modulation of El Niño/Southern Oscillation and its impacts on tropical Pacific decadal variability. *J. Climate*, *26*, 7280–7297. doi: 10.1175/JCLI-D-12-00415.1

Okumura, Y. M., & Deser, C. (2010). Asymmetry in the duration of El Niño and La Niña. *Journal of Climate*, *23*(21), 5826–5843.

Okumura, Y. M., Sun, T., & Wu, X. (2017). Asymmetric modulation of El Niño and La Niña and the linkage to tropical Pacific decadal variability. *Journal of Climate*, *30*(12), 4705–4733.

Penland, C., Flügel, M., & Chang, P., 2000. Identification of dynamical regimes in an intermediate coupled ocean–atmosphere model. *Journal of Climate*, *13*(12), 2105–2115.

Philander, S. G., & Fedorov, A. (2003). Is El Niño sporadic or cyclic? *Annual Review of Earth and Planetary Sciences*, *31*(1), 579–594.

Power, S., Casey, T., Folland, C., Colman, A., & Mehta, V. (1999). Inter-decadal modulation of the impact of ENSO on Australia. *Climate Dynamics*, *15*(5), 319–324.

Ramesh, N., & Cane, M. A. (2019). The predictability of tropical Pacific decadal variability: Insights from attractor reconstruction. *Journal of the Atmospheric Sciences*, *76*(3), 801–819.

Roberts, A., Guckenheimer, J., Widiasih, E., Timmermann, A., & Jones, C.K. (2016). Mixed–mode oscillations of El Niño–southern oscillation. *Journal of the Atmospheric Sciences*, *73*(4), 1755–1766.

Rodgers, K. B., Friederichs, P., & Latif, M. (2004). Tropical Pacific decadal variability and its relation to decadal modulations of ENSO. *Journal of Climate*, *17*(19), 3761–3774.

Santer, B. D., et al. (2014). Volcanic contribution to decadal changes in tropospheric temperature. *Nat Geosci*, *7*(3), 185–189.

Saltzman, B. (1962). Finite amplitude free convection as an initial value problem: I. *Journal of the Atmospheric Sciences*, *19*(4), 329–341.

Santoso, A., Mcphaden, M. J., & Cai, W. (2017). The defining characteristics of ENSO extremes and the strong 2015/2016 El Niño. *Reviews of Geophysics*, *55*(4), 1079–1129.

Santoso, A., Hendon, H., Watkins, A., Power, S., Dommenget, D., England, M., et al. (2019). Dynamics and predictability of El Niño–Southern Oscillation: An Australian perspective on progress and challenges. *Bull. Amer. Meteor. Soc.*, *100*(3). doi:10.1175/BAMS-D-18-0057.1

Schmidt, G. A., Shindell, D. T., & Tsigaridis, K. (2014). Reconciling warming trends. *Nat Geosci*, *7*(3), 158–160.

Schneider, N., Miller, A. J., & Pierce, D. W. (2002). Anatomy of North Pacific decadal variability. *Journal of Climate*, *15*(6), 586–605.

Schopf, P. S., & Burgman, R. J., 2006. A simple mechanism for ENSO residuals and asymmetry. *Journal of Climate*, *19*(13), 3167–3179.

Shi, J., Fedorov, A.V. and Hu, S., 2020. A Sea Surface Height Perspective on El Niño Diversity, Ocean Energetics, and Energy Damping Rates. Geophysical Research Letters, *47*(7), p.e2019GL086742.

Smith, T. M., Reynolds, R. W., Peterson, T. C. & Lawrimore, J. (2008). Improvements to NOAA's historical merged land–ocean surface temperature analysis (1880–2006). *Journal of Climate*, *21*(10), 2283–2296.

Solomon, S., Rosenlof, K. H., Portmann, R. W., Daniel, J. S., Davis, S. M., Sanford, T. J., & Plattner, G. K. (2010). Contributions of stratospheric water vapor to decadal changes in the rate of global warming. *Science*, *327*(5970), 1219–1223.

Stevenson, S., Fox-Kemper, B., Jochum, M., Neale, R., Deser, C., & Meehl, G. (2012). Will there be a significant change to El Niño in the twenty-first century? *J. Climate*, *25*, 2129–2145, doi:10.1175/JCLI-D-11-00252.1

Suarez, M. J., & Schopf, P. S. (1988). A delayed action oscillator for ENSO. *Journal of the Atmospheric Sciences*, *45*(21), 3283–3287.

Takahashi, K., & Dewitte, B. (2016). Strong and moderate non-linear El Niño regimes. *Climate Dynamics*, *46*(5–6), 1627–1645.

Thomas, M. D., & Fedorov, A. V. (2017). The eastern subtropical Pacific origin of the equatorial cold bias in climate models: A Lagrangian perspective. *Journal of Climate*, *30*(15), 5885–5900.

Thompson, C. J., & Battisti, D. S. (2000). A linear stochastic dynamical model of ENSO. Part I: Model development. *Journal of Climate*, *13*(15), 2818–2832.

Thompson, C. J., & Battisti, D. S. (2001). A linear stochastic dynamical model of ENSO. Part II: Analysis. *Journal of Climate*, *14*(4), 445–466.

Thual, S., Majda, A. J., Chen, N., & Stechmann, S. N. (2016). Simple stochastic model for El Niño with westerly wind bursts. *Proceedings of the National Academy of Sciences*, *113*(37), 10245–10250.

Timmermann, A. (1999). Detecting the nonstationary response of ENSO to greenhouse warming. *Journal of the Atmospheric Sciences*, *56*(14), 2313–2325.

Timmermann, A., Jin, F. F., & Abshagen, J. (2003). A nonlinear theory for El Niño bursting. *Journal of the Atmospheric Sciences*, *60*(1), 152–165.

Timmermann, A., et al. (2007). The influence of a weakening of the Atlantic meridional overturning circulation on ENSO. *J. Clim.*, *20*(19), 4899–4919.

Timmermann, A., An S.-I., Kug J.-S., Jin F.-F., Cai W., Capotondi A., et al. (2018). El Niño-Southern Oscillation complexity. *Nature*, *559*(7715), 535–545. doi:10.1038/s41586-018-0252-6

Trenberth, K. E., & F asullo, J. T. (2013). An apparent hiatus in global warming? *Earth's Future*. doi: 10.002/2013EF000165

Trenberth, K. E., Fasullo, J. T., Branstator, G., & Phillips, A. S. (2014). Seasonal aspects of the recent pause in surface warming. *Nature Climate Change*, *4*.

Tziperman, E., Cane, M. A., & Zebiak, S. E. (1995). Irregularity and locking to the seasonal cycle in an ENSO prediction model as explained by the quasi-periodicity route to chaos. *Journal of the Atmospheric Sciences*, *52*(3), 293–306.

Tziperman, E., Stone, L., Cane, M. A., & Jarosh, H. (1994). El Niño chaos: Overlapping of resonances between the seasonal cycle and the Pacific ocean-atmosphere oscillator. *Science*, *264*(5155), 72–74.

Vecchi, G. A., and Wittenberg, A. T. (2010). El Niño and our future climate: Where do we stand? *Wiley Interdisciplinary Reviews: Climate Change*, *1*, 260–270. doi: 10.1002/wcc.33

Vecchi, G. A., Wittenberg, A. T., & Rosati, A. (2006). Reassessing the role of stochastic forcing in the 1997–8 El Niño. *Geophys. Res. Lett.*, *33*, L01706. doi: 10.1029/2005GL024738

Vega-Westhoff, B., & Sriver, R. L. (2017). Analysis of ENSO's response to unforced variability and anthropogenic forcing using CESM. *Scientific Reports*, *7*(1), 18047.

Vimont, D. J. (2005). The contribution of the interannual ENSO cycle to the spatial pattern of ENSO-like decadal variability. *J. Climate*, *18*, 2080–2092, doi:10.1175/JCLI3365.1

Vimont, D. J., Battisti, D. S., & Hirst, A. C. (2001). Footprinting: A seasonal connection between the tropics and mid-latitudes. *Geophysical Research Letters*, *28*(20), 3923–3926.

Vimont, D. J., Wallace, J. M., & Battisti, D. S. (2003). The seasonal footprinting mechanism in the Pacific: Implications for ENSO. *Journal of Climate*, *16*(16), 2668–2675.

Wang, B. & Fang, Z. (1996). Chaotic oscillations of tropical climate: A dynamic system theory for ENSO. *Journal of the Atmospheric Sciences*, *53*(19), 2786–2802.

Wang, C., Deser, C., Yu, J. Y., DiNezio, P., & Clement, A. (2017). *El Niño and southern oscillation (ENSO): A review*. In *Coral reefs of the eastern tropical Pacific* (pp. 85–106). Springer, Dordrecht.

Watanabe, M., & Wittenberg, A. T., (2012). A method for disentangling El Niño-mean state interaction. *Geophys. Res. Lett.*, *39*, L14702. doi: 10.1029/2012GL052013

Watanabe, M., Kug, J.-S., Jin, F.-F., Collins, M., Ohba, M., & Wittenberg, A. T., (2012). Uncertainty in the ENSO amplitude change from the past to the future. *Geophys. Res. Lett.*, *39*, L20703. doi: 10.1029/2012GL053305

Watanabe, M., Shiogama, H., Tatebe, H., Hayashi, M., Ishii, M., & Kimoto, M. (2014). Contribution of natural decadal variability to global warming acceleration and hiatus. *Nat. Clim. Change*, *4*(10), 893–897.

White, S. M., Ravelo, A. C., & Polissar, P. J. (2018). Dampened El Niño in the early and mid-Holocene due to insolation-forced warming/deepening of the thermocline. *Geophysical Research Letters*, *45*(1), 316–326.

Williamson, M. S., Collins, M., Drijfhout, S. S., Kahana, R., Mecking, J. V., & Lenton, T. M. (2018). Effect of AMOC collapse on ENSO in a high resolution general circulation model. *Climate Dynamics*, *50*(7–8), 2537–2552.

Wills, R. C., Schneider, T., Wallace, J. M., Battisti, D. S., & Hartmann, D. L. (2018). Disentangling global warming, multidecadal variability, and El Niño in Pacific temperatures. *Geophysical Research Letters*, *45*(5), 2487–2496.

Wittenberg, A. T. (2002). *ENSO response to altered climates. Ph.D.* thesis, Princeton University. 475 pp. doi: 10.13140/RG.2.1.1777.8403/1

Wittenberg, A. T. (2009). Are historical records sufficient to constrain ENSO simulations? *Geophys. Res. Lett.*, *36*, L12702. doi: 10.1029/2009GL038710

Wittenberg, A. T. (2015). Low-frequency variations of ENSO. *U.S. CLIVAR Variations*, *13* (1), 26–31.

Wittenberg, A. T., Rosati, A., Lau, N.-C., & Ploshay, J. J. (2006). GFDL's CM2 global coupled climate models, Part III: Tropical Pacific climate and ENSO. *J. Climate*, *19*, 698–722. doi: 10.1175/JCLI3631.1

Wittenberg, A. T., Rosati, A., Delworth, T. L., Vecchi, G. A., & Zeng, F. (2014). ENSO modulation: Is it decadally predictable? *J. Climate*, *27*, 2667–2681. doi: 10.1175/JCLI-D-13-00577.1

Xie, S. P., Peng, Q., Kamae, Y., Zheng, X. T., Tokinaga, H., & Wang, D. (2018). Eastern Pacific ITCZ dipole and ENSO diversity. *Journal of Climate*, *31*(11), 4449–4462.

Yu, L., Weller, R. A., & Liu, T. W., (2003). Case analysis of a role of ENSO in regulating the generation of westerly wind bursts in the western equatorial Pacific. *J. Geophys. Res.*, *108*, 3128, doi:10.1029/2002JC001498.

Zanchettin, D., Bothe, O., Graf, H. F., Omrani, N.-E., Rubino, A., & Jungclaus, J. H. (2016). A decadally delayed response of the tropical Pacific to Atlantic multidecadal variability, *Geophys. Res. Lett.*, *43*, 784–792, doi:10.1002/2015GL067284

Zhao, B. and Fedorov, A., 2020. The effects of background zonal and meridional winds on ENSO in a coupled GCM. Journal of Climate, 33(6), pp.2075–2091.

Zavala-Garay, J., Zhang C., Moore A. M., Wittenberg A. T., Harrison M. J., Rosati A., et al. (2008). Sensitivity of hybrid ENSO models to unresolved atmospheric variability. *J. Climate*, *21*, 3704–3721. doi: 10.1175/2007JCLI1188.1

Zebiak, S. E., & Cane, M. A. (1987). A model El Niño–Southern Oscillation. *Monthly Weather Review*, *115*(10), 2262–2278.

Zhang, L., & Delworth, T. L. (2015). Analysis of the characteristics and mechanisms of the Pacific Decadal Oscillation in a suite of coupled models from the Geophysical Fluid Dynamics Laboratory. *Journal of Climate*, *28*(19), 7678–7701.

Zhang, L., & Delworth, T. L. (2016). Simulated response of the Pacific decadal oscillation to climate change. *Journal of Climate*, *29*(16), 5999–6018.

Zhang, R., Sutton, R., Danabasoglu, G., Delworth, T. L., Kim, W. M., Robson, J., & Yeager, S. G. (2016). Comment on "The Atlantic Multidecadal Oscillation without a role for ocean circulation." *Science*, *352*(6293), 1527–1527.